

This item is the archived peer-reviewed author-version of:

Modern tapirs as morphofunctional analogues for locomotion in endemic eocene European perissodactyls

Reference:

Maclaren Jamie, Nauwelaerts Sandra.- Modern tapirs as morphofunctional analogues for locomotion in endemic eocene European perissodactyls
JOURNAL OF MAMMALIAN EVOLUTION - ISSN 1064-7554 - (2019), p. 1-19
Full text (Publisher's DOI): <https://doi.org/10.1007/S10914-019-09460-1>
To cite this reference: <https://hdl.handle.net/10067/1580640151162165141>

1 TITLE:

2 **Modern tapirs as morphofunctional analogues for locomotion**
3 **in endemic Eocene European perissodactyls**

4 **Jamie A. MacLaren^{1*} and Sandra Nauwelaerts^{1,2}**

5

6 ¹ Department of Biology, Universiteit Antwerpen, Campus Drie Eiken, Universiteitsplein, Wilrijk,
7 Antwerp, 2610 (Belgium).

8 ² Center for Research and Conservation, Koninklijke Maatschappij voor Dierkunde (KMDA),
9 Koningin Astridplein 26, Antwerp, 2018 (Belgium).

10

11

12 * Corresponding Author

13

14

15 Corresponding Author: Jamie MacLaren, Room D.1.41, Department of Biology, Universiteit
16 Antwerpen, Campus Drie Eiken, Universiteitsplein, Wilrijk, Antwerp, 2610 (Belgium)

17

18 ORCID:

19 JM (0000-0003-4177-227X)

20 SN (0000-0002-2289-4477)

21 **Abstract**

22 Tapirs have historically been considered as ecologically analogous to several groups of extinct
23 perissodactyls based on dental and locomotor morphology. Here, we investigate comparative
24 functional morphology between living tapirs and endemic Eocene European perissodactyls to
25 ascertain whether tapirs represent viable analogues for locomotion in palaeotheres and lophiodontids.
26 Forelimb bones from 20 species of Eocene European perissodactyls were laser scanned and
27 compared to a forelimb dataset of extant *Tapirus*. Bone shape was quantified using 3D geometric
28 morphometrics; coordinates were Procrustes aligned and compared using Principal Component
29 Analysis and neighbor-joining trees. Functional traits included lever-arm ratios (LARs; proxy for
30 joint angular velocity), long-bone proportions (speed proxy), and estimated body mass. Results
31 suggest that *Paralophiodon* and *Palaeotherium magnum* resemble Neotropical tapirs in humeral
32 morphology and LARs. Palaeotheres demonstrate extensive forelimb shape disparity. Despite
33 previous assessments, metacarpal shape analyzes do not support a strong morphological similarity
34 between palaeotheres and tapirs, with *Tapirus pinchaque* representing the closest analogue for
35 Eocene European equoid manus morphology. Our analyzes suggest lophiodontids were not capable
36 of moving as swiftly as tapirs due to greater loading over the manus. We conclude that the variation
37 within modern tapir forelimb morphology confounds the assignment of one living analogue within
38 *Tapirus* for extinct European equoids, whereas tapirs adapted for greater loading over the manus
39 (e.g., *T. bairdii*, *T. indicus*) represent viable locomotor analogues for lophiodontids. This study
40 represents a valuable first step toward locomotor simulation and behavioral inference for both
41 hippomorph and tapiromorph perissodactyls in Eocene faunal communities.

42

43

44

45

46 **Keywords:**- forelimb – geometric morphometrics – lophiodontid – metacarpal – palaeothere – *Tapirus*

47 **Introduction**

48 The modern tapirs (Tapiridae: *Tapirus*) represent the crown group of a deeply rooted lineage of
49 perissodactyls (odd-toed ungulates) that diverged from their closest living relatives (rhinoceroses and
50 equids) during the earliest Eocene (approximately 56 Mya; Ryder 2009; Steiner and Ryder 2011;
51 Rose et al. 2014). The skeleton of many members of the Tapiridae (both extinct and extant)
52 demonstrates superficial similarities to the earliest ancestors of extant equoids (e.g., horses)
53 (Holbrook and Lucas 1997; Holbrook 2001; Rudwick 2008; Wood et al. 2011; Prothero 2016).
54 Similarities between tapirs and Eocene European equoids (e.g., *Eurohippus*, *Palaeotherium*) include
55 inhabiting moist, forest habitats (DeSantis and Wallace 2008; Secord et al. 2008; Zanazzi and Kohn
56 2008; Hooker 2010a; DeSantis 2011), comparable dental morphology (lophodont dentition; Simpson
57 1945; Froehlich 2002; Hulbert et al. 2009; Mihlbachler et al. 2011; Holanda and Ferrero, 2013), and
58 in many cases a tetradactyl (four-toed) forelimb (Holbrook and Lucas 1997; Prothero 2005, 2016;
59 Wood et al. 2011; Rose et al. 2014; MacLaren and Nauwelaerts 2017). The similarities in forelimb
60 morphology of the European equoid family Palaeotheriidae (palaeotheres) have in the past led to
61 tapirs being described as analogues for species within this clade (e.g., *Palaeotherium magnum* and
62 *Pa. crassum*; Cuvier 1812; Adams and Meunier 1872; Gregory 1929), with the exclusion of the
63 derived, cursorial plagiolophines. The diminutive palaeotheres *Eurohippus* and *Propalaeotherium*,
64 both of which exhibited functionally tetradactyl forelimbs (as tapirs do), have also been compared
65 with tapirs based on appearance and ecology (MacFadden 1992; Prothero 2016). However, explicit
66 quantitative data on comparisons between tapir and palaeothere functional forelimb morphology
67 (bone shape, locomotor mechanics, etc.) have not been previously published.

68

69 When establishing modern analogues for extinct taxa, understanding morphological similarities is a
70 key first step toward reconstructing locomotion of ancestral species (Thewissen and Fish 1997;

71 Carrano 1998, 1999; Hutchinson and Gatesy 2006). The close phylogenetic relationships between
72 palaeotheres and the earliest horse ancestors (e.g., *Sifrhippus*; Hooker 2010a) demonstrate that the
73 identification of a viable extant analogue for palaeothere locomotion will greatly benefit
74 investigations into modelling the transition from early tetradactyl to extant monodactyl equids
75 (Froehlich 1999, 2002; Danilo et al. 2013; Bronnert et al. 2017). Forelimb shape variation, and
76 consequent functional differences, have been described in tapirs both qualitatively and quantitatively
77 in recent years (Hulbert 2005; MacLaren and Nauwelaerts 2016, 2017; MacLaren et al. 2018). Here,
78 we will use a previously established three-dimensional forelimb dataset from extant tapirs
79 (MacLaren and Nauwelaerts 2016, 2017; MacLaren et al. 2018) and compare these to the forelimb
80 bones of Eocene European perissodactyls (including palaeotheres and contemporaneous
81 lophiodontids). Due to the tetradactyl nature of their forelimbs, we hypothesize that a three-
82 dimensional geometric morphometric analysis of bone shape will group tetradactyl Eocene equoid
83 (e.g., *Eurohippus*, *Propalaeotherium*) limb bones with those of extant tapirs, with significant
84 differences between tapirs and more derived, cursorial tridactyl palaeotheres (e.g., *Plagiolophus*, *Pa.*
85 *medium*).

86

87 Historically, ratios of forelimb and hind limb bone lengths have been used to estimate the locomotion
88 style (long-bone or ‘speed’ ratios) of extinct taxa, based on comparable ratios in living species
89 (Gregory 1929; Van Valkenburgh 1987; Samuels and Van Valkenburgh 2008). The ratios of the
90 humerus to radius (radiohumeral ratio; HR) and humerus to third metacarpal (metacarpohumeral
91 ratio; HMC) have been used to predict or demonstrate cursoriality (i.e., running locomotion) and
92 graviportalism (i.e., slow, ponderous locomotion) in quadrupedal taxa (Gregory 1929; Van
93 Valkenburgh 1987; Bai et al. 2017). Radiohumeral ratios increase with the elongation of the radius
94 (and ulna), a feature observed throughout the evolution of numerous fast-moving taxa (e.g., equids,
95 giraffes, canids; Gregory 1929; Van Valkenburgh 1987; Bai et al. 2017). The metacarpohumeral

96 ratio increases as the third metacarpal lengthens relative to the humerus; distal limb element
97 lengthening is observed in cursorial groups (e.g., equids). HMC decreases with the shortening of the
98 third metacarpal relative to the humerus, indicative of slower locomotion and higher mass over the
99 center of the manus (Gregory 1929). Here, we calculate and compare HR and HMC ratios for tapirs
100 and Eocene European perissodactyls. When these ratios are high, we expect the animal to exhibit
101 cursorial locomotor style (e.g., equids); as extant tapirs are not cursorial, we predict that tapirs will
102 be poor analogues for Eocene European perissodactyls with high HR and HMC ratios. Ultimately,
103 we reason that extant tapirs will represent a viable extant analogue for forelimb locomotion in
104 Eocene European perissodactyls that exhibit fewest significant differences in both form (limb
105 morphology; long-bone ratios) and function (lever-arm ratios; posture).

106

107 Institutional Abbreviations:– ETMNH, East Tennessee State University and General Shale Brick
108 Museum of Natural History, Gray; FSL, Geology Department of the Universite Claude Bernard
109 Lyon, Lyon; GMH, Geiseltalmuseum Halle, Halle; MNHN, Museum National d’Histoire Naturelle,
110 Paris; NHMUK, British Museum of Natural History, London; NMW, Naturhistorich Museum Wien,
111 Vienna; RBINS, Royal Belgian Institute of Natural Sciences, Brussels; SMNK, Staatliches Museum
112 fur Naturkunde Karlsruhe, Karlsruhe; ZMB MAM (MfN), Mammal Collections, Museum für
113 Naturkunde, Berlin.

114

115 **Methodology**

116 *Specimens*

117 To examine claims of morphological analogy between tapir and palaeothere locomotor anatomy,
118 forelimb bones from a range of extinct equoids and contemporaneous tapiromorphs were collected.
119 The specimens under study include several of the most well-preserved holotype postcranial remains

120 from early Eocene perissodactyls known worldwide. These were combined with many three-
121 dimensionally preserved perissodactyl forelimb bones from fossil lagerstätte such as Geiseltal
122 (Saxony-Anhalt, Germany), the Quercy Phosphorites (France), and La Debruge (Vaucluse, France).
123 Selected limb elements were scanned with a FARO ScanArm Platinum V2 system combined with an
124 integrated FARO Laser Line Probe ($\geq 50 \mu\text{m}$ resolution). Resultant models were visualized using
125 GeoMagic (GeoMagic Qualify v.10, Morrisville, NY, USA). Species studied are listed in Table 1,
126 with full details of specimens in the Supplementary Information. Tapirs represented in this analysis
127 included the four widely recognized extant *Tapirus* species (*Tapirus terrestris*, *T. pinchaque*, *T.*
128 *bairdii* and *T. indicus*; Cozzuol et al. 2013; Dumbá et al. 2018) and the dwarf *T. polkensis* from the
129 Miocene of USA. *Tapirus polkensis* was included as an approximate size analogue for several extinct
130 European perissodactyls. Eocene European perissodactyl species were scanned in museum
131 collections in France (Lyon and Paris), Germany (Karlsruhe, Berlin, and Halle), and the United
132 Kingdom (London). Fossil locality information can be found in Supplementary Fig. S5. Additional
133 specimens used for comparative limb ratios represented taxa widely considered as graviportal (e.g.,
134 teleoceratine and metamynodont rhinoceroses; *Teleoceras* spp. and *Metamynodon*) and cursorial
135 (e.g., tri- and tetradactyl equids; *Sifrihippus* and *Mesohippus* spp.) (Scott 1941; Prothero 2005; Wood
136 et al. 2011).

137

138 *Geometric Morphometrics*

139 Geometric morphometrics were used to quantify variation in shape between the forelimb bones
140 (Zelditch et al. 2012; Klingenberg 2016). A series of discrete landmark points (representing
141 biologically homologous features of the bones) were digitally placed onto each surface scan
142 (Zelditch et al. 2012) using Landmark Editor v.3.0 software (Wiley et al. 2006); landmark points
143 selected follow methods of MacLaren and Nauwelaerts (2016, 2017). Bones analyzed with 3D GM

144 included the humerus, radius, cuneiform, lunate, scaphoid, unciform, and the four metacarpals
145 (MCII, MCIII, MCIV MCV), with the remaining forelimb bones being underrepresented in all
146 extinct species in this study. Raw landmark coordinates were aligned using Generalised Procrustes
147 Analysis (GPA) (Rohlf and Slice 1990) in PAST v.3.19 (Hammer et al. 2001), removing the effects
148 of scale, location and orientation and aligning coordinate configurations based on a geometric center
149 (centroid). Aligned Procrustes coordinates from GPA were input into a Principal Components
150 Analysis (PCA) to extract the main, orthogonal axes of variation, allowing patterns of morphospace
151 occupation by different species to be compared. PCAs were performed in PAST v.3.19 (Hammer et
152 al. 2001), with principal component scores exported and visualized in morphospace plots constructed
153 in RStudio v.1.0.143 (RStudio Team 2016) using the ‘ggplot2’ library (Wickham 2009).

154

155 *Functional Traits*

156 The humerus and ulna were examined for sites of major muscular insertion pertaining to established
157 biomechanical outcomes (e.g., forearm extension; shoulder flexion) (Fig. 1a); muscles included the
158 *deltoideus*, *teres major*, *supraspinatus* and *infraspinatus* (humeral) and the lateral and long heads of
159 the *triceps brachii* (ulnar) (Fig. 1a). A series of in-lever measurements were taken between center of
160 tendon attachment and center of joint rotation, with corresponding out-lever measurements taken
161 between the center of joint rotation and the distal joint surface of the bone (recording the functional
162 length from joint to joint along the bone). Measurements were taken on 3D scans using the
163 Geomagic Studio 10 measuring tool, with ratios of out-lever over in-lever (L_o / L_i) calculated
164 following the method of Hildebrand (1985). Linear measurements were taken in three dimensions,
165 assuming perpendicular line of action to the in-lever (L_i) for all muscles. While this does not
166 necessarily represent the true line of action of the muscles in life, the methodology utilised was
167 consistent across all taxa in the analysis, allowing for legitimate functional comparisons based solely

168 on bone material. This method allowed the study of isolated and disarticulated limb elements as well
169 as articulated skeletons. Raw measurements for the in-lever and out-lever were regressed against one
170 another using ordinary least square regression (OLS), and regression plots for each muscle were
171 formatted in RStudio (RStudioTeam 2016). Regression lines for each extant tapir species were
172 compared to results from Eocene European perissodactyls and regression residuals calculated for
173 lophiodontids and palaeotheres. Regression residuals were species averaged and compared across the
174 four living taxa to test which was most analogous in its lever-arm ratios to Eocene European
175 perissodactyls.

176

177 *Long-Bone Ratios*

178 To establish whether the forelimb ratios ('locomotor ratios'; Gregory 1929) of extant tapirs
179 resembled those of Eocene European perissodactyls, the length of the humerus, radius, and third
180 metacarpal from the center of joint surfaces (representing maximum functional length) were
181 measured (Fig. 1b). Humeral, radial, and metacarpal length data from published sources (n = 10
182 species; see Table 1) were also collected and compared to measurements from scanned individuals to
183 expand species coverage for forelimb 'locomotor style' (long bone ratios; Gregory 1929; Scott 1941;
184 Radinsky 1965; Mead 2000; Prothero 2005; Franzen 2010a; Wood et al. 2011). Ratios of these
185 lengths were calculated by dividing the radius length by humerus length x 100 (HR) and third
186 metacarpal length by humerus length x 100 (HMC) (Gregory 1929; Bai et al. 2017); these ratios were
187 then species averaged. Measurements were also taken on scanned forelimbs of taxa widely believed
188 to demonstrate graviportal (e.g., *Teleoceras* spp.) and cursorial (e.g., *Mesohippus* spp.) locomotion
189 styles (22 specimens across five species), in addition to perissodactyl forelimb measurements from
190 published literature (13 specimens across nine species) (Gregory 1929; Scott 1941; Radinsky 1965;
191 Holbrook and Lucas 1997). It is important to note here that the use of ratios for parametric statistical

192 analyzes can pose issues due to certain assumptions of normality and homoscedasticity being
193 violated (Sokal and Rohlf 2012). Fortunately, several studies have shown that the use of ratio data in
194 multivariate statistics can be robust (e.g., Van Valkenburgh and Koepfli, 1993; Elissamburu and
195 Vizcano, 2004). Finally, due to the small sample sizes attained in this study, non-parametric analyzes
196 were favored; we therefore believe that the use of comparative ratio data in this study is valid. Body
197 mass was estimated from the humeri of Eocene European perissodactyls (and additional
198 perissodactyl taxa with cursorial and graviportal characteristics) using humeral width measurements
199 and regression equations from Scott (1990) (Fig. 1c), successfully applied to tapirs in recent studies
200 (Hulbert et al. 2009; MacLaren et al. 2018).

201

202 *Statistical Analyzes*

203 The first principal axes from shape-based PCA (PC1; accounting for the greatest % variance) were
204 tested for interspecific differences between taxonomic units using an analysis of variance (ANOVA)
205 and Tukey WSD (wholly significant difference) post-hoc test, both in SPSS v.24 (IBM 2013). In
206 addition, aligned Procrustes coordinates were compared across taxonomic groups using one-way
207 analysis of similarities (ANOSIM) (Clarke 1993; Warton et al. 2012). ANOSIM is a non-parametric
208 analysis that compares within-group to between-group variation and generates an R-statistic between
209 0 (equal dissimilarity between and within groups) and 1 (similarity between all within-group pairs
210 greater than any between-group pairing) (Clarke 1993). ANOSIM was conducted in RStudio using
211 the ‘vegan’ library (Oksanen et al. 2018), with pairwise comparisons of R-statistics generated in
212 PAST v.3.19.

213 Body size has been suggested to affect long-bone ratios, in addition to size affecting the
214 denomination of cursorial locomotor styles (Gregory 1929; Bai et al. 2017). To test this, long-bone
215 ratios were regressed against estimated body mass using OLS to test for a correlation between body

216 size and ‘locomotor style’ (Gregory 1929) for Eocene-Oligocene European perissodactyls and living
217 tapirs; OLS was performed in PAST v.3.19.

218 Finally, Euclidean distances between species-mean shape configurations were extracted from aligned
219 Procrustes coordinates in Morphologika v.2.5 (O’Higgins and Jones 1999) and compared using
220 neighbor-joining trees. Neighbor-joining (N-J) trees were used to heuristically visualize
221 morphological proximity of extant tapir forelimb bones to those of extinct European equoids.
222 Euclidean distances between mean long-bone ratios were also calculated to examine which tapir
223 species most closely resembled Eocene European perissodactyls in their long-bone ratio. N-J trees
224 were produced in RStudio using the ‘ape’ library (Paradis et al. 2004). [Data generated from this](#)
225 [study will be made available on reasonable request from the corresponding author; three-dimensional](#)
226 [scan data will also be available from the corresponding author with prior permission from museum or](#)
227 [institution collections managers.](#)

228

229 **Results**

230 *Forelimb Shape Variation*

231 Results of principal component analyzes (PCA) show that for each bone, certain tapir species exhibit
232 similarities in shape to specific Eocene European perissodactyls. Contrastingly, other tapir species
233 are show to exhibit significant differences in shape to one another, and to both palaeotheres and
234 lophiodontids. The first principal axis (PC1) for the long bones (humerus, radius, and metacarpals)
235 represents an axis of robusticity, with broader bones at one end of the axis and gracile bones at the
236 other end (Fig. 2) dependent upon the bone. For example, robust humeri are located in negative PC1
237 morphospace (Fig. 2a) whereas robust MCIIIIs are located in positive PC1 morphospace (Fig. 2c).
238 Lophiodontidae were excluded from metacarpal analyzes due to the scale of morphological
239 difference between this group and the others swamping interspecific differences between

240 palaeotheres and tapirs. Shape analyzes for all bones are reported in the Supplementary Fig. S1. Two
241 forelimb bones stand out as showing notable overlap between tapirs and Eocene European
242 perissodactyls: the humerus and third metacarpal (MCIII) (Fig. 2).

243 Humeral shape of tapirs overlaps along PC1 with four groups of Eocene European perissodactyls:
244 Lophiodontidae spp., *Pa. magnum*, *Pr. hassiacum*, and *Plagiolophus* spp. (Fig. 2a). Within the
245 overlapping taxa, *T. pinchaque* demonstrates overlap with *Plagiolophus* and *Pr. hassiacum*, whereas
246 all other extant tapirs and the extinct dwarf *T. polkensis* overlap with *Pa. magnum* and
247 *Paralophiodon*. No tapirs overlap with *Pr. voighti* or the basal equid *Pliolophus* along PC1 (Fig. 2a).

248 The most robust bones are found in negative PC1 morphospace, and there appear to be diagonal axes
249 of robusticity from bottom left to top right within phylogenetically separated groups: *Tapirus*
250 (squares) and palaeotheres (circles and triangles; excluding *Pliolophus*) (Fig. 2a). The landmarks
251 most greatly influencing placement along both PC1 and PC2 describe the proximodistal positioning
252 of the teres tuberosity along the humeral diaphysis, a feature that varies within *Tapirus* as well as
253 between Eocene European perissodactyls. Neighbor joining (N-J) trees confirm that mean humeral
254 landmark configurations of Lophiodontidae are most similar to extant tapirs excluding *T. pinchaque*
255 (Fig. 2b); N-J tree topology suggests that *T. pinchaque* humeri most closely resemble those of
256 *Plagiolophus* spp. ANOVA and Tukey WSD post-hoc testing suggested that *T. indicus* is separate
257 from all other tapirs and Eocene European perissodactyls; *T. terrestris* and *T. bairdii* are grouped
258 with Lophiodontidae, and *T. pinchaque* is grouped with the Palaeotheriinae taxa (Table 2). By
259 contrast, ANOSIM results suggest few similarities in humeral shape (R-statistic = 0.788); pairwise
260 R-statistic results suggest *T. pinchaque* and *T. bairdii* show the most similarities to Eocene European
261 perissodactyls (Table 3), with the lowest R-statistic recorded between *T. pinchaque* and
262 *Propalaeotherium* (R = 0.685).

263

264 Shape variation of the third metacarpal demonstrates a clear divide in morphospace between tapirs
265 and Eocene European perissodactyls, although there is a large amount of overlap along PC1 (75.1%)
266 (Fig. 2c). The slender *Pl. minor* is located in negative PC1 morphospace and the highly robust *Pa.*
267 *curtum* in positive PC1 morphospace. Landmark loadings suggest that coordinates describing
268 metacarpal narrowing dominate PC1, whereas landmarks describing the relative size and position of
269 the MCII and MCIV joint facets are highly loaded along PC2. Due to the landmarks describing
270 differences in joint facet morphology, two distinct clusters are present in morphospace: one
271 palaeothere group (Fig. 2c; top) and one tapir group (Fig. 2c; bottom right). Within these groups,
272 variation in MCIII robusticity is observed, with the most slender bones (*Plagiolophus*; *T. polkensis*
273 respectively) in the bottom left of each group and the most robust MCIIIs (*Pa. curtum*; *T. indicus*
274 respectively) found in the top right of each group (Fig. 2c). Along PC1, there is overlap between
275 tapirs (*T. polkensis*, *T. terrestris* and *T. pinchaque*) and palaeotheres (*Pr. hassiacum*, *Pa. magnum*
276 and *Pa. crassum*) (see Supplementary Fig S2 and Fig S3 for graphical species breakdown). No tapirs
277 appear in negative PC1 morphospace, which is predominated by slender tridactyl *Plagiolophus* spp.
278 and *Palaeotherium* spp. (Fig. 2c). PC2 is most greatly influenced by proximal MCIII shape and joint
279 facet arrangement. Third metacarpal N-J tree suggests that *T. pinchaque* is the most similar extant
280 tapir to Eocene European perissodactyls (*Pa. magnum* and *Pr. hassiacum*) (Fig. 2d), with the extinct
281 dwarf tapir *T. polkensis* demonstrating the most similar MCIII morphology of all the tapirs in this
282 analysis. ANOVA and Tukey WSD post-hoc tests suggest that both *T. pinchaque* and *T. terrestris*
283 MCIII mean configurations group with *Propalaeotherium* spp. (Table 2), whereas *Plagiolophus* spp.,
284 *Eurohippus* and *Palaeotherium* spp. grouping separately. When MCIII data were split into individual
285 species of *Palaeotherium* (spp. = 4) and *Plagiolophus* (spp. = 4), *T. pinchaque* and *T. terrestris*
286 grouped with *Pa. magnum*, not *Pr. hassiacum* (see Supplementary Table S1). By contrast, ANOSIM
287 results again suggest a high level of dissimilarity in MCIII shape (R-statistic = 0.836); pairwise R-
288 statistic results again suggest *T. pinchaque* demonstrates more similarities to Eocene European

289 perissodactyls (Table 3) than other living tapirs, with comparatively low R-statistics recorded
290 between *T. pinchaque* and the palaeotheres *Pa. crassum* (R = 0.741) and *Pa. magnum* (R = 0.593).
291 MCIII of tetradactyl perissodactyls in this analysis (*Tapirus* spp., *Eurohippus* and
292 *Propalaeotherium*) show much greater within-group similarity than between-group similarities (R =
293 1) (Table 3).

294

295 Results for the majority of the carpal complex of the Eocene European perissodactyls were limited
296 by specimen and species availability. Fortunately, sample size and species coverage for the unciform
297 (fourth carpal) were great enough to warrant morphological investigation. The morphological
298 variation in the unciform suggests there are three groups, separated along PC1 (Fig. 3a; Table 2). All
299 three major groups include functionally tetradactyl taxa (*Tapirus*, *Paralophiodon*,
300 *Propalaeotherium*). Lophiodontids plot separately from all other groups along PC1, overlapping with
301 extant tapirs excluding *T. pinchaque* along PC2; PC2 approximates an axis of body size.

302 Palaeotheres (including *Plagiolophus*, *Palaeotherium*, and *Propalaeotherium* spp.) group together,
303 separate from tapirs and lophiodontids (Fig. 3a; Table 2). The early tetradactyl tapiromorph
304 *Chasmothereium* occupies morphospace between the palaeothere group and the tapir group. N-J tree
305 topology suggests that *Tapirus* are clearly separate from Eocene European perissodactyls, with the
306 closest affinity to *Chasmothereium*; *Paralophiodon*, *Pa. magnum*, and *Pa. castrense* form a group
307 together, although separated by long N-J branch lengths. The unciform of Lophiodontidae possesses
308 a flattened distal facet for articulation with the fourth and fifth metacarpals, and (along with the
309 majority of the carpal bones) is proximodistally compressed when compared to the unciform of
310 *Tapirus* and palaeotheres (Fig. 3b). ANOVA and Tukey WSD post-hoc tests demonstrate the deep
311 divisions between the groups, with subsets for tapirs, *Chasmothereium* + palaeotheres (excluding
312 *Palaeotherium*), and individual subsets for *Palaeotherium* and *Paralophiodon*.

313

314 *Lever-arm Calculations*

315 Lever-arms for the muscles of the shoulder demonstrate that tapir lever arms are larger than those of
316 most Eocene European perissodactyls (Fig. 4). Individual regression lines for *T. terrestris* and
317 species averaged regression residuals between *T. terrestris* and Eocene European perissodactyls
318 suggest that this species' lever arms exhibit the closest overall affinity to those of the Eocene
319 European perissodactyls in this study (Fig. 4; Supplementary Table S2). All Eocene European
320 perissodactyls in this analysis, with the exception of *Pa. magnum*, have relatively shorter in-levers
321 for the supraspinatus than tapirs (Fig. 4a). Residuals for the supraspinatus suggest that both
322 lophiodontids and palaeotheres resemble *T. terrestris* most closely in their lever arm measurements,
323 although *T. pinchaque* and *Lophiodon* are also very similar. Regression lines and Eocene European
324 perissodactyl residuals for the infraspinatus suggest that both *T. bairdii* and *T. terrestris* are similar to
325 lophiodontids and palaeotheres (Fig. 4b; Supplementary Table S2). The only tapir that does not show
326 any close similarities to small-bodied Eocene European perissodactyls in the deltoideus is *T. indicus*
327 (similar to *Pa. magnum*), with *T. bairdii* and *T. terrestris* showing close affinity to all palaeotheres
328 (Fig. 4c). The teres major lever arm of *T. indicus* demonstrates the greatest similarity to all Eocene
329 European perissodactyls in this study excluding *Pa. magnum*, which is closest to *T. terrestris* (Fig.
330 4d). In contrast to morphological results from geometric morphometrics, *T. pinchaque* does not
331 demonstrate many close affinities to the lever arms of *Plagiolophus*, *Palaeotherium*, or
332 *Propalaeotherium* (Fig. 4; Supplementary Table S2).

333 No complete ulnae were available from *Plagiolophus* spp., *Chasmotherium*, or *Pliolophus* for
334 comparison with *Tapirus*. For the elbow muscle data available, *T. terrestris* and *T. bairdii*
335 demonstrate the closest residual distances to the lever arm results of *Propalaeotherium* and the
336 lophiodontids (Fig. 4e-f; Supplementary Table S2). The putatively cursorial *Pa. medium* represents

337 an outlier for the lever arm of the triceps brachii (long head); all Eocene European perissodactyls
338 have relatively shorter in-levers for this muscle than individuals of extant tapir species (Fig. 4f).

339

340 *Long-Bone Ratios*

341 The ratios of humerus to radius and third metacarpal lengths for Eocene European perissodactyls
342 display a broad range of measurements, demonstrating exceptionally high levels of variability within
343 the Palaeotheriidae (Fig. 5; Table 5). Long-bone ratio measurements and body mass calculations can
344 be found in Supplementary Table S3. Ratios calculated for additional taxa from published
345 measurements demonstrate low ratios for the extinct rhinocerotoids *Uintaceras*, *Metamynodon*, and
346 *Teleoceras*, all of which were notably separated from tapirs and Eocene European perissodactyls
347 (Fig. 5a; triangles). The highest ratios are recorded for the small, tridactyl palaeothere *Plagiolophus*
348 (*Pl. minor*, *Pl. annectens*), which displays long-bone ratios exceeding those of contemporaneous
349 equids (*Meshippus* spp.) and helaletids (*Colodon*) (Fig. 5a; Table 5), both of which were also
350 functionally tridactyl. The ratios displayed by extinct rhinocerotoids, helaletids, *Meshippus* spp.,
351 and *Plagiolophus* spp. were not compared to those of tapirs in subsequent analyzes to improve
352 resolution for less specialized taxa (Fig. 5b).

353 In both radio-humeral and metacarpo-humeral ratios, the tapiromorphs *Paralophiodon* and
354 *Chasmotherium* are shown to be very similar to *Tapirus* spp. (Fig. 5a-b; Table 5). *Chasmotherium*
355 (HR = 86.9; HMC = 49.9) and *T. terrestris* (86.1; 48.8) share the greatest similarity in forelimb
356 ratios, with *Paralophiodon* (87.45; 45.4) exhibiting a greater similarity to the largest tapirs *T. indicus*
357 (89.4; 47.6) and *T. bairdii* (84.6; 46.9) (Table 4). When compared to the Eocene equoids (*Hallensia*
358 + palaeotheres), both *Chasmotherium* and *Paralophiodon* are more reminiscent of tapirs in their
359 long-bone ratios. Within extant tapirs, *T. terrestris* and *T. indicus* are most similar in long-bone ratios
360 to the non-plagiolophine palaeotheres (including *Pr. hassiacum*, *E. messelensis*, and *Pa. magnum*)

361 (Fig. 5b). Despite demonstrating close similarities to Eocene perissodactyls in humeral shape, the
362 long humerus of *T. pinchaque* causes low HR and HMC ratios when compared to other tapirs. As a
363 result, this taxon does not show close affinities to Eocene European perissodactyls in their long-bone
364 ratios. The extinct dwarf *T. polkensis* displays similar long-bone ratios to those of *Hallensia*, *Pr.*
365 *voigti*, and the extinct helaetid *Heptodon*; this tapir is not close to any living tapirs in the proportions
366 of its long forelimb elements. The basal equid *Sifrhippus* exhibits comparable metacarpo-humeral
367 ratios to those of extant tapir species; this taxon also displays a radio-humeral ratio intermediate
368 between the tetradactyl palaeotheres *Eurohippus* and *Propalaeotherium* (Fig. 5b). OLS regression
369 and permutation of long-bone ratios against log-transformed body mass estimates demonstrate
370 significant negative correlation between mass and radiohumeral ($r = -0.70$; $r^2 = 0.49$; $p < 0.01$) and
371 metacarpohumeral ($r = -0.72$; $r^2 = 0.51$; $p < 0.01$) ratios for available taxa.

372

373 **Discussion**

374 In this study we used various quantitative approaches to test whether extant species of tapir (*Tapirus*)
375 represent viable morphological and functional forelimb analogues for Eocene European
376 perissodactyls. Previous qualitative comparisons have suggested that the limbs of tapirs
377 morphologically resemble those of species within the tridactyl genus *Palaeotherium* (including *Pa.*
378 *magnum* and *Pa. crassum*) (Cuvier 1812; Adams and Meunier 1872; Rudwick 2008), with additional
379 comparisons drawn to the tetradactyl Lophiodontidae and *Propalaeotherium* in overall biology
380 (Agusti and Anton 2004; Franzen 2010b; Prothero 2016). Here, we demonstrate that no one extant
381 tapir species is a viable analogue for Eocene European perissodactyls; however, several individual
382 tapir species show both morphological and functional attributes of the forelimb that would make
383 them viable analogues for locomotion in certain groups of Eocene European perissodactyls. Using a
384 combination of morphological similarities (quantified using geometric morphometrics), forelimb

385 proportion comparisons (long-bone ratios), and joint functional morphology (lever-arm ratio
386 comparisons), we discuss how variable Eocene European perissodactyl limb morphology is, and how
387 these respective morphologies and associated functions compare to living tapir analogues.

388

389 *Locomotor diversity within Palaeotheriinae*

390 In recent studies, tapirs have been demonstrated to display significant differences in forelimb
391 morphology pertaining to specific functional outcomes (MacLaren and Nauwelaerts 2016, 2017).
392 However, this diversity in form and function is meager when compared to the diversity in forelimb
393 morphology displayed by the Palaeotheriidae. The results of this study categorically support the
394 earliest descriptions of palaeotheres diverging greatly in their forelimb bone morphology from one
395 another (Cuvier 1812; Rudwick 2008), highlighted by the disparity observed in both the radius and
396 third metacarpal (Fig. 2 and Fig. 6; Supplementary Fig. S1).

397 The Palaeotheriidae include both tetradactyl and tridactyl members (Agusti and Anton 2004; Franzen
398 2006, 2010b; Danilo et al. 2013), and as a result may be expected to demonstrate a high degree of
399 morphological variation in the forelimb. The first descriptions of palaeotheres are those of the
400 currently recognized Palaeotheriinae (Cuvier 1812), a monophyletic clade which includes the genera
401 *Palaeotherium* and *Plagiolophus* (Danilo et al. 2013; Remy 2015; Bai 2017). These two genera are
402 both functionally tridactyl palaeothere clades; however, despite their close phylogenetic affinity, they
403 demonstrate high morphological diversity within the forelimb (Figs 2, 5 and 6). Shape variation in
404 the third metacarpal of the most variable genus, *Palaeotherium*, is shown to be far greater than
405 exhibited by any other in this study, including *Tapirus* (Fig. 2 and Fig. 6). Several contemporaneous
406 palaeotheriines exhibited diverse manus dimensions (e.g., *Pa. curtum* and *Pl. minor*; Fig. 6),
407 implying a range of locomotor behaviors (e.g., cursoriality) and potentially accompanying variation
408 in ecological niche. As observed by Cuvier, *Pa. curtum* possesses highly robust forelimb bones,

409 indicative of a heavily built taxon, whereas *Plagiolophus* spp. and *Pa. medium* demonstrate elongate
410 and gracile metacarpals, akin to their equid cousins (Cuvier 1812; MacFadden 2005; Franzen 2010b).
411 Despite this divergence in morphology, the metacarpals of *Pa. curtum* and *Pl. minor* are of
412 approximately equal absolute length. A comparable situation is observed in many other perissodactyl
413 communities, including the Miocene of Florida (*Nannipus* (Equidae) and *Aphelops* (Rhinocerotidae);
414 Love Bone Bed) and France (*Anchitherium* (Equidae) and *Hoploaceratherium* (Rhinocerotidae);
415 Sansan) (MacFadden and Hulbert 1990; Alberdi and Rodriguez 2012; Heissig 2012). Palaeotheriines
416 diversified to occupy many available locomotor niches, potentially pertaining to specific partitioning
417 of resources based on taxon mobility. The short and stout manus of *Pa. curtum*, coupled with a
418 comparatively long but robust radius (Fig. 6), is reminiscent of the basal rhinoceros *Uintaceras*
419 (Holbrook and Lucas 1997), described as exhibiting multiple features of a graviportal existence (e.g.,
420 highly robust limb bones; femur much longer than tibia; Holbrook and Lucas 1997). The
421 plagiolophines and *Pa. medium*, with their elongated distal forelimbs and posteriorly curved radii and
422 ulnae (Fig. 6), would have represented a cursorial group of palaeotheres. The diminutive
423 plagiolophines (e.g., *Pl. minor*), with small body size and elongate forelimb morphology represent
424 the only members of the clade to survive through the Eocene-Oligocene extinction event (the
425 ‘Grande Coupure’)(Joomun et al. 2008; Hooker 2010b). The climatic changes throughout Eurasia
426 during this extinction event are hypothesized to have favored animals adapted to drier, more open
427 habitats (Blondel 2001). In addition to differential dietary specializations compared to other late
428 Eocene palaeotheres (Joomun et al. 2008), the elongated limbs and reduced body size may have
429 benefitted plagiolophines in drier, open habitats in Europe immediately following the ‘Grande
430 Coupure’ (Blondel 2001; Hooker 2010b). These cursorial adaptations would allow small browsers to
431 rapidly flee from predators in more open terrain where shelter may have been scarce. In contrast, the
432 more graviportal palaeotheres (e.g., *Pa. curtum*) did not attain the sizes that contemporaneous North
433 American browsing perissodactyls (e.g., brontotheres) achieved, and their truncated manus and

434 robust upper limbs would not have been favorable for swift escape or efficient movement over longer
435 distances in the more open environments of Oligocene Europe.

436

437 *Cursorial palaeothere shoulder analogy*

438 The comparisons drawn between tapir forelimb anatomy and that of palaeotheres in previous studies
439 (e.g., Cuvier, 1812) have been demonstrated to warrant re-evaluation in this study. First, any
440 comparisons of the putatively cursorial palaeotheres (*Plagiolophus* and *Pa. medium*) to tapirs in
441 terms of their locomotor anatomy and function may be considered erroneous, on the evidence of this
442 study. The long-bone ratios of *Plagiolophus* (Fig. 5), coupled with the large size difference between
443 this genus and all *Tapirus* in this analysis (Fig. 4), suggest that locomotor analogy between these taxa
444 and tapirs is unlikely. Conversely, the lever-arm similarities between the palaeotheres *Plagiolophus*
445 and *Propalaeotherium* and the extant *T. terrestris* (Figs. 4 and 7; Supplementary Table S2)
446 demonstrate that the muscular action on the shoulder and elbow in this tapir may indeed be
447 representative of the functional morphology in smaller palaeotheres. There is also a noteworthy
448 similarity in teres major lever-arm ratio between *T. indicus* and all the Eocene European
449 perissodactyls in the analysis (Fig. 4d). The site of insertion for this muscle (the teres tuberosity of
450 the humerus) is a discriminant feature for living tapirs (MacLaren and Nauwelaerts 2016), suggestive
451 of interspecific differences within tapirs in mechanical action of the teres major and latissimus dorsi
452 muscles, both of which insert on the tuberosity. The variation in placement of the teres tuberosity
453 along the shaft of the humerus in *Plagiolophus*, *Palaeotherium* cf. *medium*, and *Propalaeotherium* is
454 akin to the range observed in living *Tapirus* species. The placement of the lateral humeral flexor (the
455 deltoideus) in the smaller Eocene European perissodactyls (*Propalaeotherium* and *Plagiolophus*)
456 coupled with comparatively longer in-lever measurements is more reminiscent of the large *T. indicus*
457 than any other living tapir (Fig. 4c and Fig. 7).

458 Based on our understanding of how morphometric features scale with changes in mass (Biewener
459 2003, 2005), the similarities in flexor insertions and lever-arm measurements between the cursorial
460 palaeotheres (20-80kg) and the more massive *T. terrestris* (~220kg) and *T. indicus* (~325kg) suggest
461 that muscles acting on the shoulder of cursorial palaeotheres (e.g., *Plagiolophus*) were
462 disproportionately smaller relative to those of extant tapirs. This means that the muscle mass around
463 the shoulder would have been very limited, giving the shoulder region of smaller cursorial
464 palaeotheres a very gracile appearance akin to small antelopes, chevrotains, and goats (Gewaily et al.
465 2017). Interestingly, juvenile members of *T. indicus* demonstrate shoulder flexor insertions
466 approximately central to the humeral diaphysis (MacLaren, pers. obs.), as is observed in cursorial
467 palaeotheres. It is, therefore, possible that the functional morphology of the juvenile *T. indicus*
468 forelimb would be of greater comparative value for small palaeotheres than that of the much larger
469 adult.

470

471 *Corroborating Cuvier on palaeothere morphology*

472 Whereas many palaeotheres in this analysis are small, presenting a number of scaling issues to
473 consider when drawing conclusions on locomotor analogy, there is one taxon which approximates
474 living tapir species in both size and shape: *Palaeotherium magnum* (Table 4). This taxon was
475 described by Cuvier as displaying strong similarities to tapirs in the metacarpus, which we
476 corroborate and expand upon with this quantitative analysis. Similarities in MCIII shape between the
477 mountain tapir *T. pinchaque* and *Pa. magnum* were observed (PCA and ANOSIM results; Fig. 2;
478 Table 3), and are likely driven by the comparatively broad metacarpophalangeal joint facet in *Pa.*
479 *magnum* when compared to other tridactyl palaeotheres (Fig. 6; Palaeotheriinae), and the more
480 slender profile of the MCIII in *T. pinchaque* (MacLaren and Nauwelaerts 2017). This is also true for
481 the palaeothere *Pa. crassum*, described in the past as “resembling a tapir even more than [*Pa.*

482 *magnum*], for it did not differ in its size and proportions” (Cuvier 1812; translation from Rudwick
483 2008). By contrast, we find that *Pa. magnum* resembles tapirs more closely than *Pa. crassum* (for the
484 bones available for the latter species), principally due to the more gracile shape of the metapodials
485 and radius in *Pa. crassum*. Therefore, from this point on our morphofunctional comparison focuses
486 upon *Pa. magnum*.

487 From a functional standpoint, results from body mass estimation and lever-arm ratios suggest that
488 *Pa. magnum* may have demonstrated similar muscle mass in the shoulder and upper forelimb region
489 to both *T. indicus* and *T. terrestris* (Table 4; Fig. 4). Other large tapirs with longer limbs not included
490 in this study (e.g., *T. webbi*; Hulbert 2005; MacLaren et al. 2018) may represent a closer proportional
491 analogue for *Pa. magnum* within *Tapirus*; however, as this taxon is itself extinct, it cannot represent
492 a viable living analogue for modelling locomotion in this large palaeothere. It is therefore difficult to
493 isolate one individual tapir species that shows ideal morphofunctional similarities to *Pa. magnum*.

494 First of all, every tapir living today retains all four digits in the manus, whereas *Pa. magnum* (and all
495 other palaeotheriines) have reduced their MCV to a non-functional vestige (Cuvier 1812). The more
496 gracile metacarpal morphology of *T. pinchaque* is shown to be similar to that of *Pa. magnum* (Table
497 3); however, this is countered by the proximal shift in muscle insertions on the humerus of this tapir,
498 whereas the upper limb functional morphology of *T. indicus* or *T. terrestris* appears an ideal
499 analogue. The obligate reliance on the lateral fifth digit in *T. indicus* (and the consequent
500 morphological changes in the carpus; Earle 1893; Simpson 1945; MacLaren and Nauwelaerts 2017)
501 rule this tapir out as a model species for a functionally tridactyl *Pa. magnum* (Table 4; Fig. 3).

502 Therefore, we conclude that, due to close similarities in humeral shape and lever-arms, metacarpal
503 shape, predicted body mass, and only facultative use of the lateral MCV, the closest locomotor
504 analogue for *Pa. magnum* within living tapirs is the lowland tapir *T. terrestris*. Any future
505 mechanical modelling undertaken on *Palaeotherium* should naturally account for the differences in
506 the manus morphology and spread of loading forces when compared to the tetradactyl tapir.

507

508 *Lack of tetradactyl palaeothere analogy*

509 The earliest European perissodactyls were (to our knowledge) all functionally tetradactyl; these
510 include taxa such as *Lophiodon* and *Paralophiodon* (Holbrook 2009), *Eurohippus*, *Propalaeotherium*
511 (Franzen 2010a), *Hallensia*, and *Chasmotherium* (Radinsky 1967; Franzen 1990; Remy 2015).
512 Functional tetradactyly is present in palaeotheres, albeit in the smaller and more primitive forms
513 (e.g., *Propalaeotherium*). Evidence from this study suggests that the morphology of the metacarpals
514 and lateral carpus in tetradactyl palaeotheres more closely resembles that of tridactyl palaeotheres
515 (Fig. 2c-d, Fig. 3a), in some cases those of much greater size (e.g., *Propalaeotherium* and *Pa.*
516 *magnum*; Fig. 2c, Table 4). In living tapirs, the unciform carpal and both third and fourth metacarpals
517 have been shown to demonstrate morphological differences relating to the functional use of the fifth
518 (most lateral) digit. The MCIII is elongate relative to the MCIV in tapirs with reduced lateral
519 metacarpal usage (e.g., *T. bairdii*, *T. terrestris*; Earle, 1893; MacLaren and Nauwelaerts 2017), and
520 the MCIV also exhibits a flattened joint facet with the unciform in species reliant on the MCV for
521 locomotion (e.g., *T. indicus*). The unciform also demonstrates morphological variability across
522 *Tapirus*, both in keeping with greater loading of the fifth metacarpal (Earle 1893; Simpson 1945;
523 MacLaren and Nauwelaerts 2017) and with habitat density (MacLaren et al. 2018). The distribution
524 of loading forces through the carpus therefore appears to be more similar within phylogenetically
525 related groups than between perissodactyls exhibiting functional tetradactyly. In addition, the
526 relatively long and thin fifth metacarpal of tetradactyl palaeotheres has no extant equivalent in
527 ungulates, and is more reminiscent of the manus arrangement in felids or canids (Barone 2000). This
528 apparent phylogenetic constraint on morphology in the manus, and notable size difference as
529 mentioned earlier, makes the assignment of a living analogue for tetradactyl palaeotheres within the
530 tapirs difficult. Although metacarpal shape and upper forelimb lever-arms are suggestive of
531 similarities between *Propalaeotherium* and *T. terrestris* (Figs. 2c and 4), we feel that assigning this

532 tapir as a viable locomotor analogue for *Propalaeotherium* would require a substantial over-
533 interpretation of the data available.

534

535 *Locomotion in the Lophiodontidae*

536 Living contemporaneously alongside palaeotheres, the lophiodontids represent an enigmatic extinct
537 group of tetradactyl perissodactyls endemic to Europe that have been compared to tapirs based upon
538 general appearance and feeding ecology (Depéret 1907; Holbrook 2001; Agusti and Anton 2004;
539 Franzen 2010b). In this study we find that the morphology of the humerus of lophiodontids
540 (*Paralophiodon leptorhynchum* and *Lophiodon tapirotherium*) cannot be statistically separated from
541 *T. terrestris* or *T. bairdii* (Table 2), although between-group variation is greater than that of almost
542 all living tapirs (Table 3). The humerus of *Lophiodon* exhibits a prominent deltoid tuberosity and a
543 proximodistally long teres tuberosity (Holbrook 2009), implying that the deltoideus and teres major
544 (shoulder flexor) act slightly differently to those of living tapirs. The lateral projection of the deltoid
545 tuberosity increases the mechanical advantage of the deltoideus, which acts as the primary lateral
546 shoulder flexor. In addition, the olecranon process of the ulna is rounded in lateral aspect (as
547 observed in *T. indicus*; MacLaren and Nauwelaerts, 2016) and also in caudal aspect; this increases
548 surface area insertion potential for the long head of the triceps brachii, one of the major limb
549 extensors involved in gravitational support (Liebich et al. 2007). This large, rugose insertion site is
550 mirrored by evidence of similarly robust origination sites for the triceps on lophiodontid scapulae
551 (Holbrook 2009). The implication of these muscle attachment morphologies, similar in many ways to
552 those of rhinoceros, hippopotamus, and elephant humeral flexors (Depéret 1907; Prothero 2005;
553 Fisher et al. 2007), is that the lophiodontids possessed a highly muscularized upper arm, ideal for
554 supporting large masses over the forelimb (Prothero 2005). With regards to the carpus and
555 metacarpals of lophiodontids (principally represented by *Paralophiodon* in this study; see

556 Supplementary Fig. S1), a similar suite of load-bearing adaptations are observed. *Paralophiodon*
557 exhibits several features indicative of comparatively greater loading being applied over the forelimb
558 than in living tapirs. First, the proximal row of carpals (scaphoid, lunate, and cuneiform) demonstrate
559 a large degree of proximodistal compression compared to those of most extant tapirs and
560 palaeotheres. Within recent tapirs, the Central American *T. bairdii* has been shown to demonstrate
561 compressed proximal carpals relative to other tapirs (MacLaren and Nauwelaerts 2017); due to the
562 decreased reliance on the fifth digit in this taxon, proximal carpal compression was interpreted as an
563 adaptation to higher loading over the manus compared to *T. terrestris* or *T. pinchaque* (Prothero
564 2005; MacLaren and Nauwelaerts 2017). We find a similar condition in *Paralophiodon*, albeit with
565 more extreme proximal carpal compression and more greatly reduced fifth metacarpal in the type
566 manus of *Paralophiodon leptorhynchum* (FSL 2685), as described by Deperet (1907) and Holbrook
567 (2009). Evidence of carpal compression is further observed in the distal carpal row (unciform,
568 magnum, and trapezoid) (Fig. 3), most markedly in the unciform. The unciform demonstrates a near-
569 flattened distal joint facet for interaction with the fourth and fifth digits (MCIV and MCV) (Fig. 3b).
570 The flattened distal facet spreads compressive forces across the fourth and fifth metacarpals during
571 the stance phase of locomotion in *Paralophiodon*. This morphology is not observed in tapirs or
572 tetradactyl palaeotheres, which both exhibit a convex distal unciform joint for the MCIV (MacLaren
573 and Nauwelaerts 2017). Ultimately, this suggests that the MCIV, at least of *Paralophiodon*, was
574 more heavily loaded than that of either tapirs or tetradactyl palaeotheres (Earle 1893; Gregory 1929;
575 Simpson 1945; Prothero 2005; MacLaren and Nauwelaerts 2017). Interestingly, a similar condition is
576 observed in the carpus of the pygmy hippopotamus *Hexaprotodon* (*Choeropsis*); although excluded
577 from this study, the potential ecological and locomotor comparisons between lophiodontids and the
578 artiodactyl *Hexaprotodon* are an ideal avenue of future investigation.

579 *Paralophiodon* is well known from multiple isolated specimens from the middle Eocene deposits at
580 La Livinière (Depéret 1907; Buffetaut 1986; Martin 2014) (Lutetian, possibly Bartonian in age).

581 Among the specimens incorporated in this study, two distinct fifth metacarpals (MCVs) were found;
582 one belonging to the type manus FSL 2685, the other misidentified as a second metacarpal (MCII) in
583 another associated manus (FSL 2686). The MCV of FSL 2686 is distinctly longer (+33%) than that
584 of the type manus for *Paralophiodon*; this bone does not cluster with the MCV from the type
585 specimen, but is in fact closer to the MCVs of Eocene-Oligocene rhinocerotoids and the relatively
586 cursorial Miocene tapir *T. polkensis* (Supplementary Fig. S1f). On the premise that tapiromorph
587 metacarpals do not differ greatly in length relative to one another through ontogeny (MacLaren, pers.
588 obs.), and that tapiromorphs do not exhibit significant osteological shape differences between sexes
589 (despite demonstrating sexual dimorphism in size; Simpson 1945; Mead 2000), we interpret FSL
590 2686 as likely representing a different species from the same locality. A thorough phylogenetic
591 examination of all postcranial elements will be necessary to establish this with any certainty. At this
592 point, the presence of this bone in the deposits of La Livinière indicates the likely presence of
593 another species of lophiodontid alongside *Paralophiodon leptorhynchum*, which appears to
594 demonstrate an alternative locomotor niche (functional tetradactyly). Ecologically, the early Eocene
595 locality of La Livinière is well known for terrestrial crocodylians, small artiodactyls, and creodonts,
596 indicative of a drier and more terrestrial habitat than other deposits harboring lophiodontid remains
597 (Martin 2014). This represents a similar habitat to that preferred by the living tapirs *T. terrestris* and
598 *T. bairdii* (Bodmer and Brooks 1997; Matola et al. 1997). The short lateral metacarpal of
599 *Paralophiodon* (based on the type manus) is notably reminiscent of the patterns of metacarpal length
600 observed in *T. bairdii* (MacLaren and Nauwelaerts 2017). Combined, we therefore conclude that the
601 compressed proximal carpal row, reduced fifth metacarpal, lever-arm ratios, and forelimb
602 proportions indicate that the most suitable extant locomotor analogue for *Paralophiodon* within
603 tapirs is the Central American tapir *T. bairdii*.

604 It should be noted that lophiodontids demonstrate a large range of mass and shape in the forelimb,
605 although many of these bones were not suitable for analysis in this study. To test whether

606 *Paralophiodon* differs in locomotor ecology to other lophiodontids found in deposits suggesting a
607 moist-habitat (e.g., *Lophiodon remensis* from Monthelon, France (Smith et al. 2004); *L.*
608 *tapirotherium* from Geiseltal, Germany (Holbrook 2009)), further three-dimensional quantification
609 of multiple lophiodontid taxa will be necessary, with the aid of retrodeformation of severely crushed
610 remains (e.g., *L. lautricense*).

611

612 **Conclusions**

613 In this study we have successfully quantified forelimb variation in Eocene European perissodactyls
614 which, in previous literature, have been compared in their morphology and ecology to extant tapirs.
615 This geometric morphometric study clearly highlights the extreme variation in Eocene European
616 perissodactyl locomotor morphology. To assign a closest extant analogue within *Tapirus* to (for
617 example) the genus *Palaeotherium* would consequently be impossible given the variation in form
618 (limb morphology) and function (e.g., rapid vs. slow shoulder flexion) of the forelimb in Eocene
619 European perissodactyls. The plesiomorphic, yet variable, forelimb of *Tapirus* certainly demonstrates
620 similarities in both form and function when compared to some palaeotheres and lophiodontids, as
621 previously noted (albeit qualitatively) by Cuvier and Depéret during the early descriptions of these
622 Eocene taxa (Cuvier 1812; Depéret 1907). Tapir upper forelimb morphology, lever-arms, and limb
623 proportions suggest the closest analogy to members of the Lophiodontidae (e.g., *Paralophiodon*
624 *leptorhynchum*), which are here shown to be more variable in their locomotor ecology than
625 previously observed. The greatest similarities between extant tapirs and lophiodontids are shown
626 between *Paralophiodon* and the Central American tapir *Tapirus bairdii*. The Lophiodontidae may
627 exhibit as much variation in form as is present in palaeotheres, although it was not possible to
628 include all taxa in this study due to extensive taphonomic modification of many limb bones (Depéret
629 1907; Holbrook 2009; Robinet et al. 2015). When compared to the highly diverse palaeotheres, tapirs

630 with more gracile metapodials (e.g., *T. pinchaque*, *T. polkensis*) are shown to be morphologically
631 more similar. In confirmation of Cuvier's work on palaeotheres (Cuvier 1812; Rudwick 2008), both
632 *Pa. magnum* and *Pa. crassum* are demonstrated to resemble tapirs in their overall forelimb
633 morphology (most closely that of *T. pinchaque*). The question of scaling will always be of
634 importance when comparing extant and extinct species in search of potential analogy; in this case,
635 both *Pa. crassum* and *Pa. magnum* approximate living tapirs in their estimated size, further
636 supporting historical claims of morphofunctional similarity. In contrast to the speculations of Cuvier,
637 the 'cursorial palaeotheres' *Pa. medium* and *Plagiolophus* spp. show few similarities to any tapir
638 species in this study, beyond similarities in flexor lever-arms acting on the shoulder. This is
639 indicative of a similar shoulder muscle application and function between palaeotheres and tapirs, but
640 also that the greatest modifications in palaeothere forelimb morphology exist in the distal segments
641 (as is the case in equids; MacFadden 1992) rather than the proximal segments (as evidenced in living
642 tapirs; MacLaren and Nauwelaerts 2016). This study has endeavored to utilize recent techniques and
643 understanding of tapir functional locomotor morphology (MacLaren and Nauwelaerts 2016 2017;
644 MacLaren et al. 2018) to cast light on the locomotion of poorly understood Eocene European
645 perissodactyls. Future work incorporating other potential analogues (e.g., *Hexaprotodon*, suids, etc.)
646 and combining morphometrics with ecological data (e.g., tooth micro/mesowear, stable isotopes,
647 cranial and lumbar mechanics) will enable these bizarre clades to be better understood as members of
648 Eocene European ecosystems, and facilitate a more fundamental understanding of adaptive radiations
649 within perissodactyl clades.

650

651 **Acknowledgements:** The authors wish to thank the following: M. Stache, F. Steinheimer and O.
652 Wings (GMH), T. Schosleitner (MfN), G. Billet (MNHN), P. Brewer, J. Hooker and S. Pappa
653 (NHMUK), A. Folie and T. Smith (RBINS), E. Frey (SMNK), and E. Robert (FSL) for access to
654 Eocene European perissodactyl specimens; all curatorial staff at the AMNH, ETMNH, MfN,

655 MNHN, MVZ, NMW, and RMNH for access to tapir specimens; J. Mertens, J. Meany-Ward and J.
656 Scholliers for logistical support; H. Hanegraef, P. Indekeu and C. Mallet for scanning assistance; and
657 L. Holbrook, J. Hooker and P. Aerts for guidance on interpretations and manuscript writing. This
658 work was funded by an FWO doctoral scholarship and EAVP Travel Grant (JM) and a BOF-UA
659 grant (SN).

660

661 **References**

- 662 Adams WHD, Meunier V (1872) The Pachydermata. In: Adams WHD, Meunier V, (eds) Life in the
663 Primeval World. T. Nelson and Sons, New York, pp 107-142
- 664 Agusti J, Anton M (2004) The Eocene: Reaching the Climax. In: Mammoths, Sabertooths, and
665 Hominids: 65 Million Years of Mammalian Evolution in Europe. Columbia University Press,
666 New York, pp 23-66
- 667 Alberdi MT, Rodriguez J (2012) *Anchitherium* Meyer, 1844 (Perissodactyla, Equidae) de Sansan. In:
668 Peigné S, Sen S (eds) Mammifères de Sansan. Publication Scientifiques du Museum, Paris,
669 pp 487-533
- 670 Bai B (2017) Eocene Pachynolophinae (Perissodactyla, Palaeotheriidae) from China, and their
671 palaeobiogeographical implications. *Palaeontology* 60:837–852
- 672 Bai B, Meng J, Wang Y-Q, Wang H-B, Holbrook LT (2017) Osteology of the middle Eocene
673 ceratomorph *Hyrachyus modestus* (Mammalia, Perissodactyla). *Bull Am Mus Nat Hist*
674 413:1–70
- 675 Barone R (2000) Muscles de la ceinture et du membre thoraciques. In: Anatomie Comparée Des
676 Mammifères Domestique. Editions Vigot, Paris, pp 719–842
- 677 Biewener AA (2005) Biomechanical consequences of scaling. *J Exp Biol* 208:1665–1676

- 678 Biewener AA, Patek SN (2018) Movement on land. In: Animal Locomotion. Oxford University
679 Press, Oxford, pp 61-89
- 680 Blondel C (2001) The Eocene-Oligocene ungulates from Western Europe and their environment.
681 Palaeogeogr Palaeoclimatol Palaeoecol 168:125–139
- 682 Bodmer RE, Brooks DM (1997) Status and action plan of the lowland tapir (*Tapirus terrestris*). In:
683 Brooks DM, Bodmer RE, Matola S (eds) Tapirs: Status Survey and Conservation Action
684 Plan. IUCN/SSC Tapir Specialist Group, Cambridge, pp 46–56
- 685 Bronnert C, Gheerbrant E, Godinot M, Métais G (2017) A primitive perissodactyl (Mammalia) from
686 the early Eocene of Le Quesnoy (MP7, France). Hist Biol 30:237–250
- 687 Buffetaut É (1986) Un Mésosuchien ziphodonte dans l'Éocène supérieure de La Livinière (Hérault,
688 France). Geobios 19:101–113
- 689 Carrano MT (1998) Locomotion in non-avian dinosaurs: integrating data from hindlimb kinematics,
690 in vivo strains, and bone morphology. Paleobiology 24:450–469
- 691 Carrano MT (1999) What, if anything, is a cursor? Categories versus continua for determining
692 locomotor habit in mammals and dinosaurs. J Zool 247:29–42
- 693 Clarke KR (1993) Non-parametric multivariate analyzes of changes in community structure. Austral
694 Ecol 18:117–143
- 695 Cozzuol MA, Clozato CL, Holanda EC, Rodrigues FHG, Nienow S, de Thoisy B, Redondo RAF,
696 Santos FR (2013) A new species of tapir from the Amazon. J Mammal 94:1331–1345
- 697 Cuvier G (1812) Recherches sur les ossemens fossiles de quadrupèdes: Tome III. Chez Deterville
698 Libraire, Paris

699 Danilo L, Remy JA, Vianey-Liaud M, Marandat B, Sudre J, Lihoreau F (2013) A new Eocene
700 locality in southern France sheds light on the basal radiation of Palaeotheriidae (Mammalia,
701 Perissodactyla, Equoidea). *J Vertebr Paleontol* 33:195–215

702 Depéret MC (1907) Études des Membres du *Lophiodon*. In: Depéret MC (ed) Études
703 Paléontologiques Sur Les *Lophiodon* Du Minervois: Structure Du Cran, Des Membres et
704 Affinités Générales Des *Lophiodon*. A. Rey and Company, Lyon., pp 34–40

705 DeSantis LRG (2011) Stable isotope ecology of extant tapirs from the Americas. *Biotropica* 43:746–
706 754

707 DeSantis LRG, Wallace SC (2008) Neogene forests from the Appalachians of Tennessee, USA:
708 geochemical evidence from fossil mammal teeth. *Palaeogeogr, Palaeoclimatol, Palaeoecol*
709 266:59–68

710 [Dumbá LCCS, Dutra RP, Cozzuol MA \(2018\) Cranial geometric morphometric analysis of the genus](#)
711 [Tapirus \(Mammalia, Perissodactyla\). *J Mammal Evol* doi.org/10.1007/s10914-018-9432-2](#)

712 Earle C (1893) Some points in the comparative osteology of the tapir. *Science* 21:118

713 Elissamburu A, Vizcaíno SF (2004) Limb proportions and adaptations in caviomorph rodents
714 (Rodentia: Caviomorpha). *J Zool* 262:145–159

715 Fisher REK, Scott M, Naples VL (2007) Forelimb myology of the pygmy hippopotamus
716 (*Choeropsis liberiensis*). *Anat Rec* 290:673–693

717 Franzen JL (1990) *Hallensia* (Mammalia, Perissodactyla) aus Messel und dem Pariser Becken sowie
718 Nachtrage aus dem Geiseltal. *Bulletin de l’Institut Royal des Sciences Naturelles de*
719 *Belgique, Sciences de la Terre* 60:175–201

720 Franzen JL (2006) *Eurohippus* n.g., a new genus of horses from the middle to late Eocene of Europe.
721 *Senckenbergiana Lethaea* 86:97–102

- 722 Franzen JL (2010a) The dawn horses of the morning cloud. In: The Rise of Horses: 55 Million Years
723 of Evolution. Johns Hopkins University Press, Baltimore, pp 45–76
- 724 Franzen JL (2010b) Pseudo horses and relatives of horses. In: The Rise of Horses: 55 Million Years
725 of Evolution. Johns Hopkins University Press, Baltimore, pp 145–164
- 726 Franzen JL, Hauptzeter J (2017) Complete skeleton of *Eurohippus messelensis* (Mammalia,
727 Perissodactyla, Equoidea) from the early middle Eocene of Grube Messel (Germany).
728 *Palaeobio Palaeoenv* 97:807–832
- 729 Froehlich DJ (1999) Phylogenetic systematics of basal perissodactyls. *J Vertebr Paleontol* 19:140–
730 159
- 731 Froehlich DJ (2002) *Quo vadis eohippus?* The systematics and taxonomy of the early Eocene equids
732 (Perissodactyla). *Zool J Linn Soc* 134:141–256
- 733 Gewaily MS, Fayed MH, Farrag FA (2017) Architectural and functional specifications of the
734 intrinsic muscles of the forelimb of the Egyptian Baladi goats (*Capra hircus*). *Alexandria J*
735 *Vet Sci* 55:110–124
- 736 Gregory WK (1929) Mechanics of locomotion in the evolution of limb structure as bearing on the
737 form and habits of the titanotheres and the related odd-toed ungulates. In: Osborn HF (ed)
738 The Titanotheres of Ancient Wyoming, Dakota and Nebraska. United States Government
739 Printing Office, Washington D.C., pp 727–756
- 740 Hammer Ø, Harper DAT, Ryan PD (2001) PAST: paleontological statistics software package for
741 education and data analysis. *Palaeontol Electron* 4:9
- 742 Heissig K (2012) Les Rhinocerotidae (Perissodactyla) de Sansan. In: Peigné S, Sen S (eds)
743 Mammifères de Sansan. Publication Scientifiques du Museum, Paris, pp 317–486

- 744 Hildebrand M (1985) Walking and running. In: Hildebrand DB, Bramble M, Liem DM, Wake KF
745 (eds) Functional Vertebrate Morphology. Harvard University Press, Cambridge, pp 38–57
- 746 Holanda EC, Ferrero BS (2013) Reappraisal of the genus *Tapirus* (Perissodactyla, Tapiridae):
747 systematics and phylogenetic affinities of the South American tapirs. *J Mammal Evol* 20:33–
748 44
- 749 Holbrook LT (2001) Comparative osteology of early Tertiary tapiromorphs (Mammalia,
750 Perissodactyla). *Zool J Linn Soc* 132:1–54
- 751 Holbrook LT (2009) Osteology of *Lophiodon* Cuvier, 1822 (Mammalia, Perissodactyla) and its
752 phylogenetic implications. *J Vertebr Paleontol* 29:212–230
- 753 Holbrook LT, Lucas SG (1997) A new genus of rhinocerotoid from the Eocene of Utah and the
754 status of North American “*Forstercooperia*.” *J Vertebr Paleontol* 17:384–396
- 755 Hooker JJ (2010a) The mammal fauna of the early Eocene Blackheath Formation of Abbey Wood,
756 London. *Monograph of the Palaeontographical Society* 624:1–162
- 757 Hooker JJ (2010b) The “Grande Coupure” in the Hampshire Basin, UK: taxonomy and stratigraphy
758 of the mammals on either side of this major Paleogene faunal turnover. In: Whittaker JE,
759 Hart MB (eds) *Micropalaeontology, Sedimentary Environments and Stratigraphy: A Tribute*
760 *to Dennis Curry (1912-2001)*. The Geological Society Publishing House, Bath, pp 147–215
- 761 Hulbert RC (2005) Late Miocene *Tapirus* (Mammalia, Perissodactyla) from Florida, with description
762 of a new species, *Tapirus webbi*. *Bull Florida Mus Nat Hist* 45:465–494
- 763 Hulbert RC, Wallace SC, Klippel WE, Parmalee PW (2009) Cranial morphology and systematics of
764 an extraordinary sample of the Late Neogene dwarf tapir, *Tapirus polkensis* (Olsen). *J*
765 *Paleontol* 83:238–262
- 766 Hutchinson JR, Gatesy SM (2006) Beyond the bones. *Nature* 440:292–294

767 IBM Corp. (2017) IBM SPSS Statistics for Windows, Version 25.0. Armonk, NY. IBM Corp.

768 Joomun SC, Hooker JJ, Collinson ME (2008) Dental wear variation and implications for diet: an
769 example from Eocene perissodactyls (Mammalia). *Palaeogeogr Palaeoclimatol Palaeoecol*
770 263:92–106

771 Klingenberg CP (2016) Size, shape, and form: concepts of allometry in geometric morphometrics.
772 *Development Genes and Evolution* 226:113–137

773 Liebich H-G, König HE, Maierl J (2007) Forelimb or thoracic limb (membra thoracica). In: König
774 HE, Liebich H-G (eds) *Veterinary Anatomy of Domestic Animals: Textbook and Color*
775 *Atlas*. Schlutersche, Stuttgart, pp 145–214

776 MacFadden BJ (1992) What's the use? Functional morphology of feeding and locomotion. In: *Fossil*
777 *Horses: Systematics, Paleobiology, and Evolution of the Family Equidae*. Cambridge
778 University Press, Cambridge, pp 229–262

779 MacFadden BJ (2005) Fossil horses – evidence for evolution. *Science* 307:1728–1730

780 MacFadden BJ, Hulbert RC (1990) Body size estimates and size distribution of ungulate mammals
781 from the late Miocene Love Bone Bed of Florida. In: Damuth J, MacFadden BJ (eds) *Body*
782 *Size in Mammalian Paleobiology: Estimation and Biological Implications*. Cambridge
783 University Press, Cambridge, pp 337–363

784 MacLaren JA, Nauwelaerts S (2016) A three-dimensional morphometric analysis of upper forelimb
785 morphology in the enigmatic tapir (Perissodactyla: *Tapirus*) hints at subtle variations in
786 locomotor ecology. *J Morphol* 277:1469–1485

787 MacLaren JA, Nauwelaerts S (2017) Interspecific variation in the tetradactyl manus of modern tapirs
788 (Perissodactyla: *Tapirus*) exposed using geometric morphometrics. *J Morphol* 278:1515–
789 1535

790 MacLaren JA, Hulbert RC, Wallace SC, Nauwelaerts S (2018) A morphometric analysis of the
791 forelimb in the genus *Tapirus* (Perissodactyla: Tapiridae) reveals influences of habitat,
792 phylogeny and size through time and across geographical space. *Zool J Linn Soc.* 184:499–
793 515

794 Martin JE (2014) A sebecosuchian in a middle Eocene karst with comments on the dorsal shield in
795 Crocodylomorpha. *Acta Palaeontol Pol* 60:673–680

796 Matola S, Cuarón AD, Rubio-Torgler H (1997) Status and action plan of the Baird's tapir (*Tapirus*
797 *bairdii*). In: Brooks DM, Bodmer RE, Matola S (eds) *Tapirs: Status Survey and Conservation*
798 *Action Plan*. IUCN/SSC Tapir Specialist Group, Cambridge, pp 29–45

799 Mead AJ (2000) Sexual dimorphism and paleoecology in *Teleoceras*, a North American Miocene
800 rhinoceros. *Paleobiology* 26:689–706

801 Mihlbachler MC, Rivals F, Solounias N, Semprebon GM (2011) Dietary change and evolution of
802 horses in North America. *Science* 331:1178–1181

803 O'Higgins P, Jones N (1999) *Morphologika. Tools for Shape Analysis*. University College London,
804 London.

805 Oksanen J, Blanchet FG, Friendly M, Kindt R, Legendre P, McGlinn D, Minchin PR, O'Hara RB,
806 Simpson GL, Solymos P, Stevens MHH, Szoecs E, Wagner H (2018) *vegan: Community*
807 *Ecology Package*. R package vers 2.5-3

808 Paradis E, Claude J, Strimmer K (2004) *APE: Analyzes of Phylogenetics and Evolution in R*
809 *language*. *Bioinformatics* 20:289–290

810 Prothero DR (2005) Postcranial osteology. In: *The Evolution of North American Rhinoceroses*.
811 Cambridge University Press, Cambridge, pp 146–181

- 812 Prothero DR (2016) Perissodactyla. In: Prothero DR (ed) The Princeton Guide to Prehistoric
813 Mammals. Princeton University Press, Oxford, pp 186–202
- 814 Radinsky LB (1965) Evolution of the tapiroid skeleton from *Heptodon* to *Tapirus*. Bull Mus Comp
815 Zool 134:69–106
- 816 Radinsky LB (1967) *Hyrachyus*, *Chasmothorium*, and the early evolution of helaletid tapiroids. Am
817 Mus Novitates 2313:1–23
- 818 Remy JA (1992) Observations sur l’anatomie crânienne du genre *Palaeotherium* (Perissodactyla,
819 Mammalia); mise en évidence d’un nouveau sous-genre, *Franzenitherium*. Palaeovertebrata
820 21:105–221
- 821 Remy JA (2015) Les Périssodactyles (Mammalia) du gisement Bartonien supérieur de Robiac
822 (Éocène moyen du Gard, Sud de la France). Palaeovertebrata 39:1–99
- 823 Robinet C, Remy JA, Laurent Y, Danilo L, Lihoreau F (2015) A new genus of Lophiodontidae
824 (Perissodactyla, Mammalia) from the early Eocene of La Borie (southern France) and the
825 origin of the genus *Lophiodon* Cuvier, 1822. Geobios 48:25–38
- 826 Rohlf FJ, Slice D (1990) Extensions of the Procrustes method for the optimal superimposition of
827 landmarks. Syst Zool 39:40–59
- 828 Rose KD, Holbrook LT, Rana RS, Kumar K, Jones KE, Ahrens HE, Missiaen PE, Sahni A, Smith T
829 (2014) Early Eocene fossils suggest that the mammalian order Perissodactyla originated in
830 India. Nat Comm 5:5570
- 831 RStudioTeam (2016) RStudio: Integrated Development for R.
- 832 Rudwick MJS (2008) The animals from the Gypsum Beds around Paris. In: Rudwick MJS (ed)
833 George Cuvier, Fossil Bones and Geological Catastrophes: New Translations and
834 Interpretations of the Primary Texts. University of Chicago Press, Chicago, pp 59–67

- 835 Ryder OA (2009) Rhinoceroses, tapirs, and horses (Perissodactyla). In: Hedges SB, Kumar S (eds)
836 The Timetree of Life. Oxford University Press, Oxford, pp 508–510
- 837 Samuels JX, Van Valkenburgh B (2008) Skeletal indicators of locomotor adaptations in living and
838 extinct rodents. *J Morphol* 269:1387–1411
- 839 Scott KM (1990) Postcranial dimensions of ungulates as predictors of body size. In: Damuth J,
840 MacFadden BJ (eds) *Body Size in Mammalian Paleobiology: Estimation and Biological*
841 *Implications*. Cambridge University Press, Cambridge, pp 301–335
- 842 Scott WB (1941) The mammalian fauna of the White River Oligocene: Part V. Perissodactyla. *Trans*
843 *Am Philo Soc New Ser* 28:747–964
- 844 Secord R, Wing SL, Chew A (2008) Stable isotopes in early Eocene mammals as indicators of forest
845 canopy structure and resource partitioning. *Paleobiology* 27:539–563
- 846 Simpson GG (1945) Notes on Pleistocene and recent tapirs. *Bull Am Mus Nat Hist* 86:33–82
- 847 Smith T, De Wilde B, Steurbaut E (2004) Primitive equoid and tapiroid mammals: keys for
848 interpreting the Ypresian-Lutetian transition in Belgium. *Bulletin de l’Institut Royal des*
849 *Sciences Naturelles de Belgique, Sciences de la Terre* 74:165–175
- 850 Sokal RR, Rohlf FJ (2012) *Biometry: The Principles and Practice of Statistics in Biological*
851 *Research*. W. H. Freeman and Co., New York.
- 852 Steiner CC, Ryder OA (2011) Molecular phylogeny and evolution of the Perissodactyla. *Zool J Linn*
853 *Soc* 163:1289–1303
- 854 Thewissen JGM, Fish FE (1997) Locomotor evolution in the earliest cetaceans: functional model,
855 modern analogues, and paleontological evidence. *Paleobiology* 23:482–490

856 Van Valkenburgh B (1987) Skeletal indicators of locomotor behavior in living and extinct
857 carnivores. *J Vertebr Paleontol* 7:162–182

858 Van Valkenburgh B, Koepfli K (1993) Cranial and dental adaptations to predation in canids. *Symp*
859 *Zool Soc Lond* 65:15–37

860 Warton DI, Wright ST, Wang Y (2012) Distance-based multivariate analyzes confound location and
861 dispersion effects. *Methods Ecol Evol* 3:89–101

862 Wickham H (2009) *Ggplot2: Elegant Graphics for Data Analysis*. Springer, New York

863 Wiley DF, Amenta N, Alcantara DA, Ghosh D, Kil YJ, Delson E, Harcourt-Smith W, Rohlf FJ, St.
864 John K, Hamann B, Motani R, Frost S, Rosenberger AL, Tallman L, Disotell T, O’Neill R
865 (2006) *Landmark Editor 3.0*. Institute for Data Analysis and Visualization (IDAV) and the
866 University of California, Davis

867 Wood AR, Bebej RM, Manz CL, Begun DL, Gingerich PD (2011) Postcranial functional
868 morphology of *Hyracotherium* (Equidae, Perissodactyla) and locomotion in the earliest
869 horses. *J Mammal Evol* 18:1–32

870 Zanzazi A, Kohn MJ (2008) Ecology and physiology of White River mammals based on stable
871 isotope ratios of teeth. *Palaeogeogr Palaeoclimatol Palaeoecol* 257:22–37

872 Zelditch ML, Swiderski DL, Sheets HD (2012) *Geometric Morphometrics for Biologists: A Primer*.
873 Elsevier Academic Press, New York

874

875

876

877

878 **Figure Captions**

879 **Fig. 1** Measurement techniques for forelimb functional trait calculation. (a) (from left) diagram
880 representing the shoulder and elbow musculature; color-coded muscles with key; insertions sites in
881 lateral aspect with action of muscles on the shoulder and elbow joints shown in arrows (black = joint
882 flexion; white = joint extension); example of in-lever (black) and out-lever (white) measurements
883 (for deltoideus). (b) Maximum length from center of joint articulation (functional length) of humerus
884 (left), radius, and third metacarpal (right) for long-bone ratios. Bones not to scale; (c) humeral width
885 measurements for body mass estimations.

886

887 **Fig. 2** Morphological comparison of humerus (a, b) and third metacarpal (c, d) between *Tapirus*
888 species and extinct European perissodactyls. Principal components 1 and 2 demonstrate variation in
889 shape (a, c), with associated neighbor-joining trees based on Euclidean distances between species
890 mean landmark configurations (b, d). Approximate bone shapes based on PC1 variation shown
891 (bottom). Location of bones shown on scanned forelimb of *Propalaeotherium hassiacum* (top right).
892 Shape key: circles = Palaeotheriinae; triangles = other Palaeotheriidae + *Pliolophus*; square =
893 Tapiridae; diamond = Lophiodontidae.

894

895 **Fig. 3** Comparison of unciform morphology between *Tapirus* spp. and European Eocene
896 perissodactyls. (a) Principal components 1 and 2 demonstrate variation in shape between the groups;
897 (b) genus level comparison between *Tapirus* and *Lophiodon* unciform morphology, with unciform-
898 metacarpal joint facet highlighted. Silhouettes represent skeletal forelimbs of *Tapirus bairdii* (top)
899 and *Lophiodon* (excluding phalanges). Shape key: circles = Palaeotheriinae; triangles = other
900 Palaeotheriidae; square = Tapiridae.

901

902 **Fig. 4** Lever-arm comparison of upper forelimb bones of *Tapirus* species with extinct European
903 perissodactyls. In-lever lengths plotted against out-lever for supraspinatus (a), infraspinatus (b),
904 deltoideus (c), teres major (d); lateral (e) and long (f) head of triceps brachii. OLS regression line for
905 individual tapir species best fitting extinct European perissodactyl pattern shown. Insertion sites and
906 action of muscles (arrows) shown on forelimb diagram (right): black arrows = shoulder, white
907 arrows = elbow; bones of left forelimb in lateral view. Shape key: circles = tridactyl Palaeotheriidae;
908 triangles = tetradactyl Palaeotheriidae; square = Tapiridae; diamond = Lophiodontidae.

909

910 **Fig. 5** Long-bone ratio comparison of *Tapirus* spp. and selected extinct perissodactyls. (a) Radio-
911 humeral (HR) and metacarpo-humeral (HMC) ratios plotted against one another. (b) Neighbor-
912 joining trees based on distances between mean ratios for extant *Tapirus* and European perissodactyls
913 (excluding *Plagiolophus* spp.). Dotted lines mark approximate boundary between cursorial and
914 mediportal long-bone ratios, according to Gregory (1929). Silhouettes represent taxa demonstrating
915 typically graviportal (Rhinocerotidae: *Teleoceras*) and cursorial (Palaeotheriinae: *Plagiolophus*) limb
916 ratios.

917

918 **Fig. 6** Variation of locomotor morphology across Palaeotheriidae. Radius (left) and third metacarpal
919 shown for three clades of Palaeotheriidae alongside tapirs for comparison; bones not to scale.
920 Unrooted phylogeny based on Remy (1992) and Danillo et al. (2013). Silhouettes represent exemplar
921 bauplans for each group. Abbreviations: tet = tetradactyl; tri = functionally tridactyl.

922

923

924

925 **Fig. 7** Variation of muscular insertion sites on the humerus of tapirs and Eocene European
926 perissodactyls. Humeri of tapirs (a-d) shown alongside three palaeothere taxa (e-g) in lateral view.
927 Black bar represents midpoint of the humeral shaft. Muscular insertions: supraspinatus (red);
928 infraspinatus (green); deltoideus (blue); teres major (medial insertion; white). In particular note
929 variation in teres major and deltoid insertions across *Tapirus* and between Eocene European
930 perissodactyls.

931

932

933

934

935

936

937

938

939

940

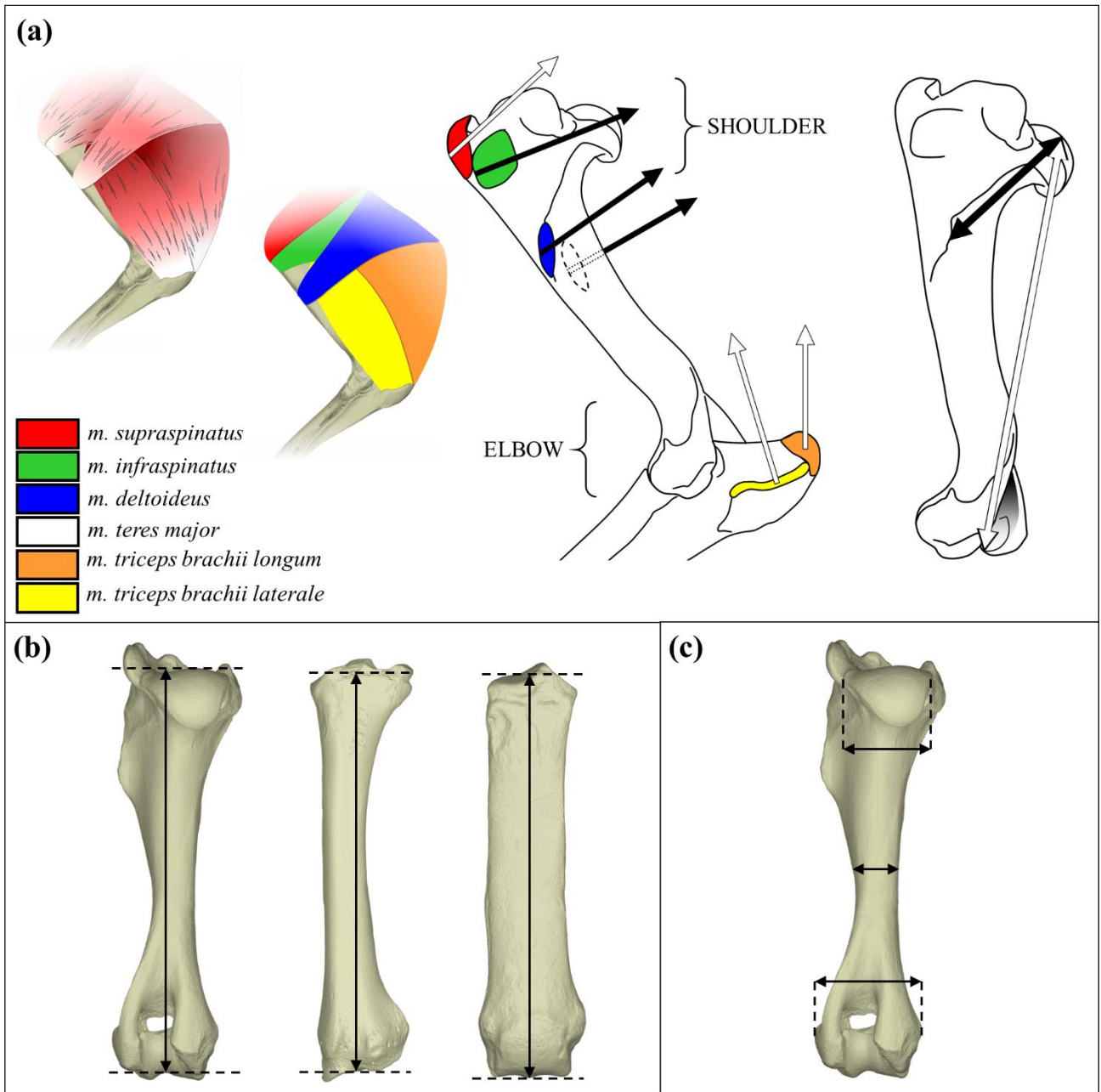
941

942

943

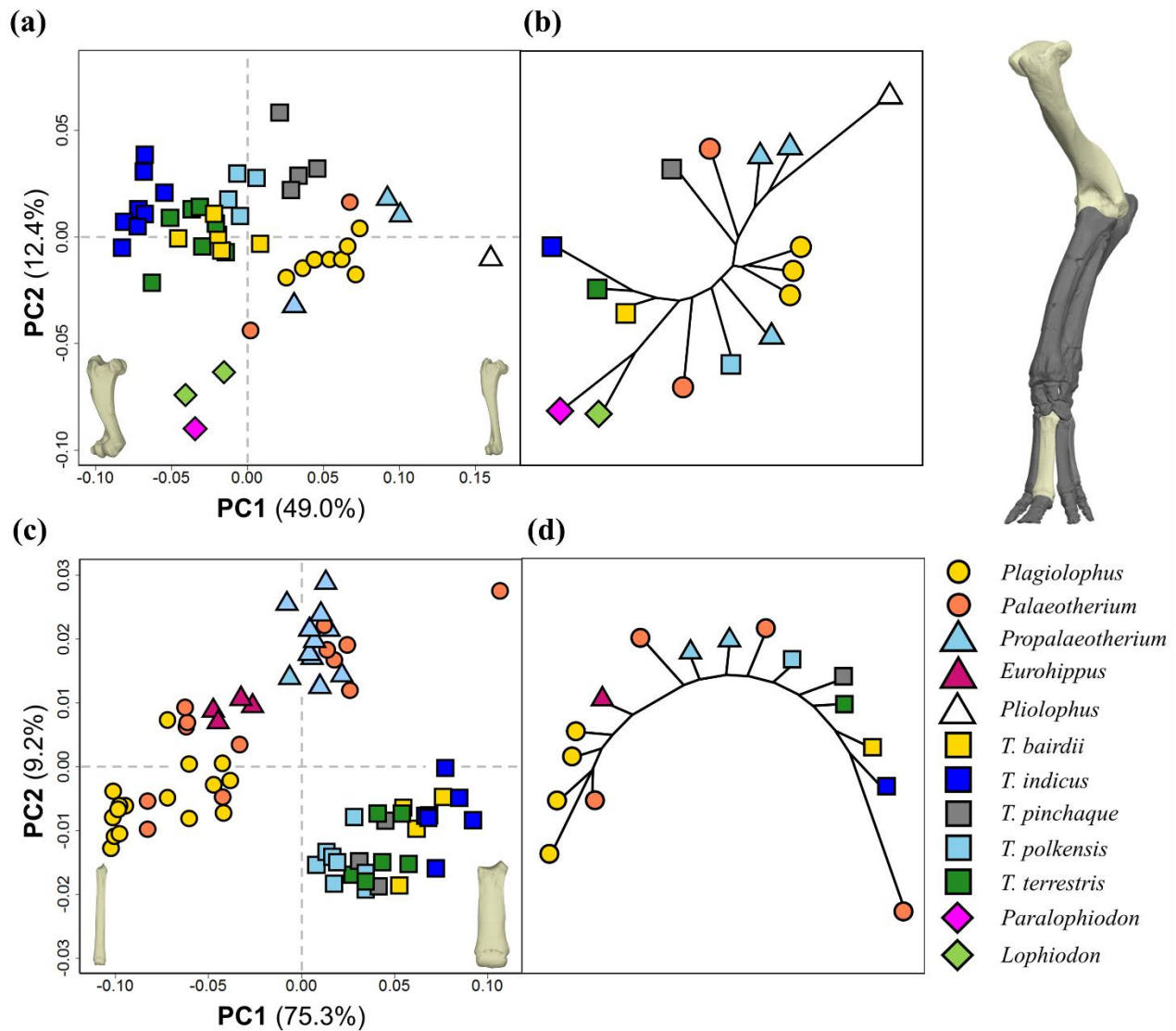
944

945



946

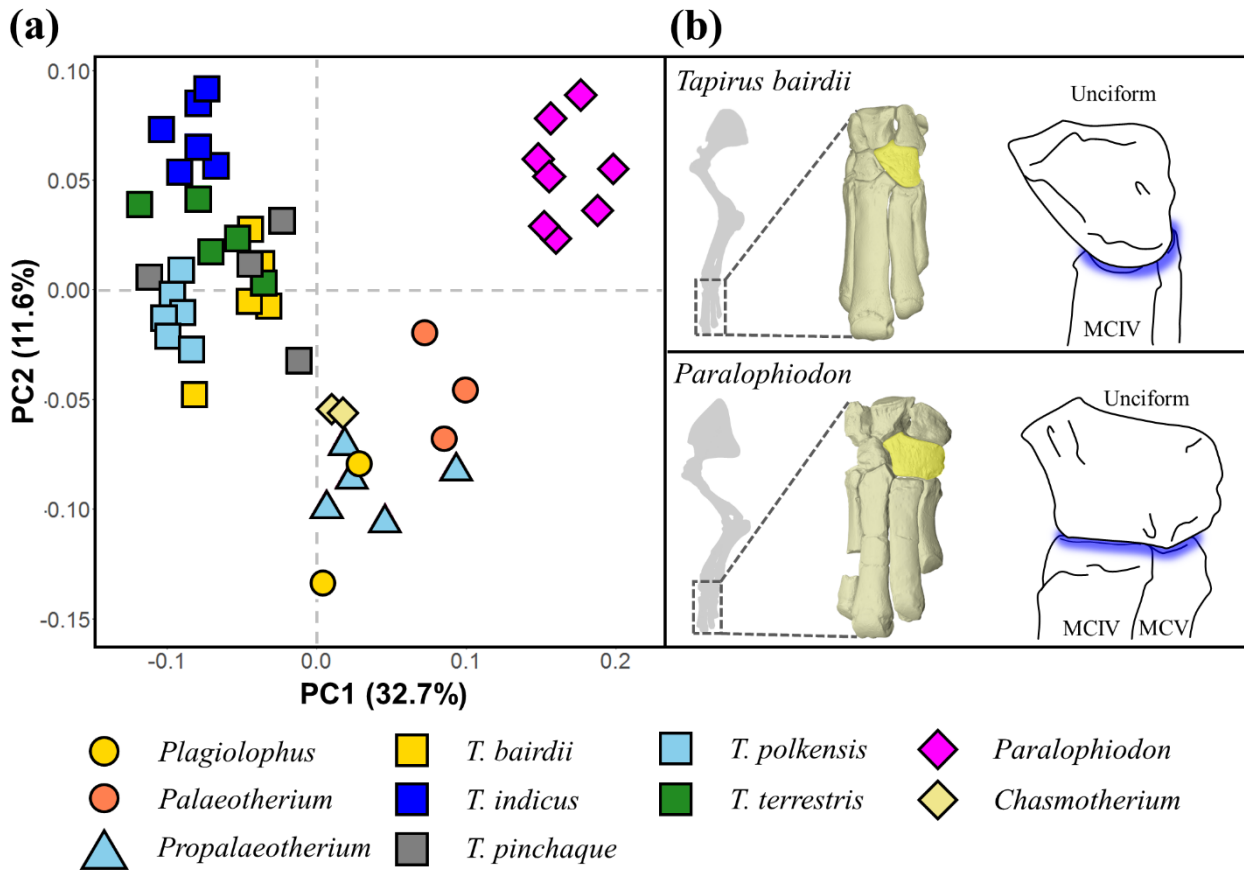
947 **Figure 1.** Measurement techniques for forelimb functional trait calculation. **(a)** (from left) diagram
 948 representing the shoulder and elbow musculature; colour-coded muscles with key; insertions sites in
 949 lateral aspect with action of muscles on the shoulder and elbow joints shown in arrows (black = joint
 950 flexion; white = joint extension); example of in-lever (black) and out-lever (white) measurements
 951 (for *m. deltoideus*). **(b)** Maximum length from centre of joint articulation (functional length) of
 952 humerus (left), radius and third metacarpal (right) for long-bone ratios. Bones not to scale; **(c)**
 953 humeral width measurements for body mass estimations.



954

955 **Figure 2.** Morphological comparison of humerus (a, b) and third metacarpal (c, d) between *Tapirus*
 956 species and extinct European perissodactyls. Principal components 1 and 2 demonstrate variation in
 957 shape (a, c), with associated neighbour-joining trees based on Euclidean distances between species
 958 mean landmark configurations (b, d). Approximate bone shapes based on PC1 variation shown
 959 (bottom). Location of bones shown on scanned forelimb of *Propalaeotherium hassiacum* (top right).
 960 Shape key: circles = Palaeotheriinae; triangles = other Palaeotheriidae + *Pliolophus*; square =
 961 Tapiridae; diamond = Lophiodontidae.

962



963

964 **Figure 3.** Comparison of unciform morphology between *Tapirus* spp. and European Eocene
 965 perissodactyls. **(a)** Principal components 1 and 2 demonstrate variation in shape between the groups;
 966 **(b)** genus level comparison between *Tapirus* and *Lophiodon* unciform morphology, with unciform-
 967 metacarpal joint facet highlighted. Silhouettes represent skeletal forelimbs of *Tapirus bairdii* (top)
 968 and *Lophiodon* (excluding phalanges). Shape key: circles = Palaeotheriinae; triangles = other
 969 Palaeotheriidae; square = Tapiridae.

970

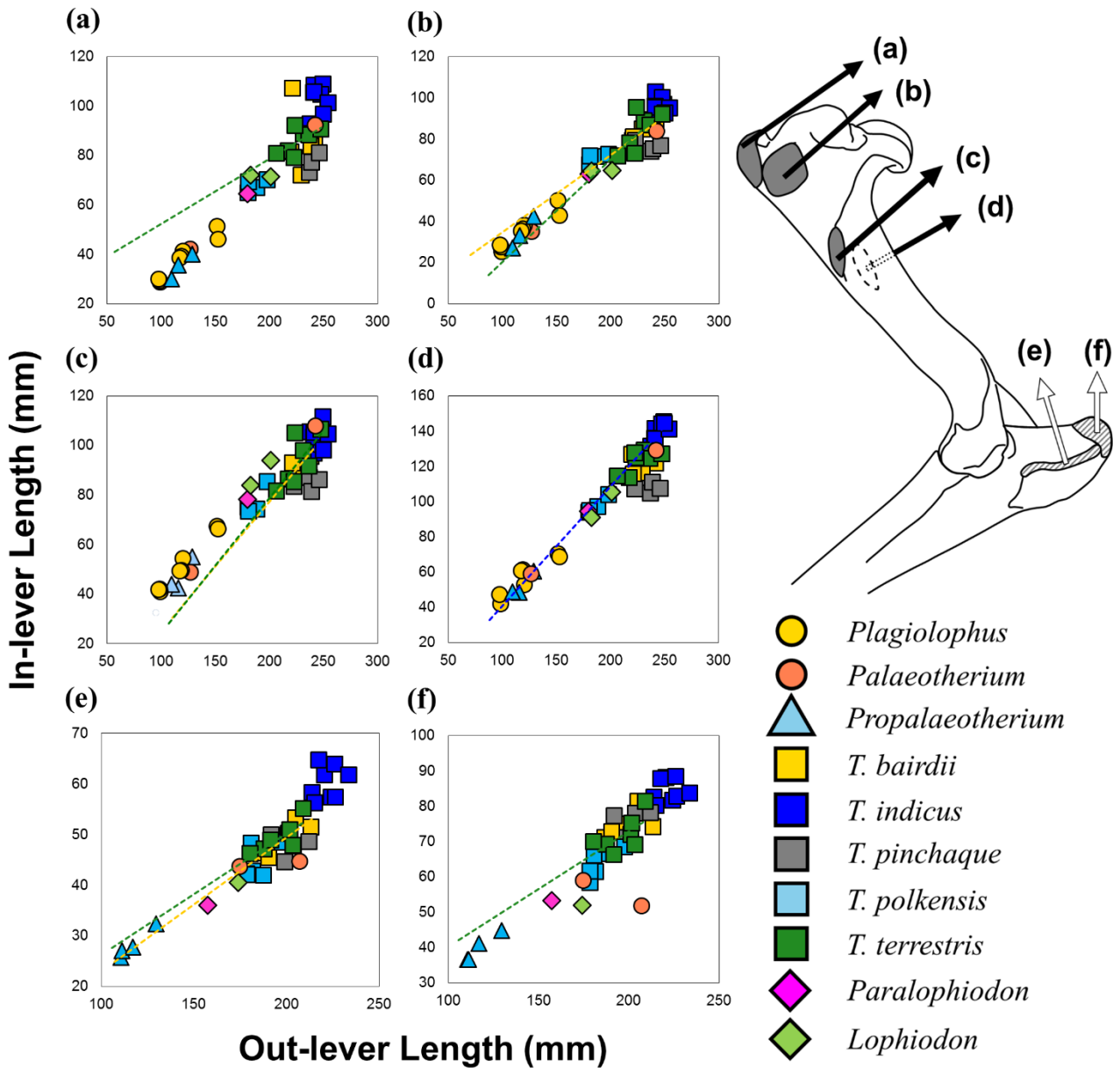
971

972

973

974

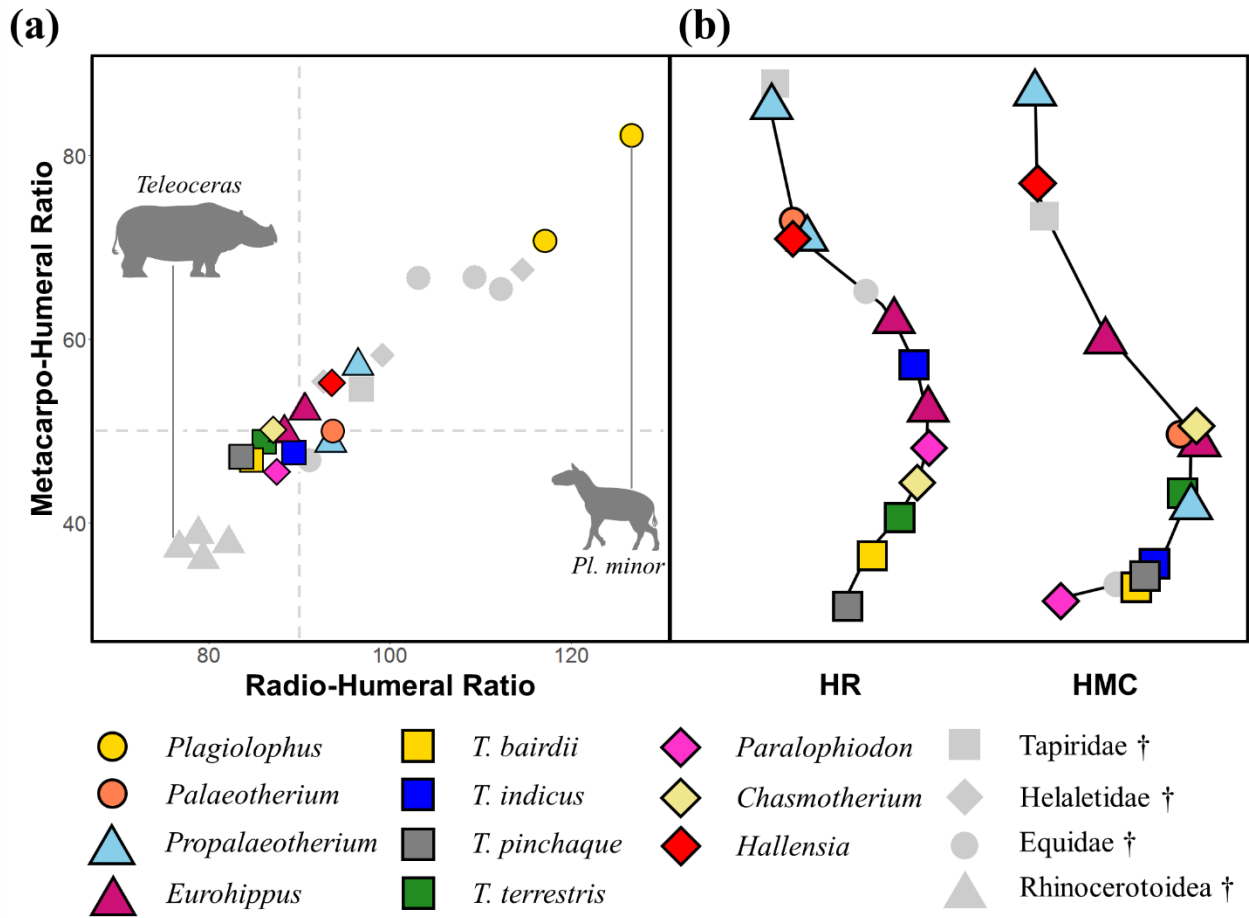
975



976

977 **Figure 4.** Lever-arm comparison of upper forelimb bones of *Tapirus* species with extinct European
 978 perissodactyls. In-lever lengths plotted against out-lever for *supraspinatus* (a), *infraspinatus* (b),
 979 *deltoideus* (c), *teres major* (d); lateral (e) and long (f) head of *triceps brachii*. OLS regression line for
 980 individual tapir species best fitting extinct European perissodactyl pattern shown. Insertion sites and
 981 action of muscles (arrows) shown on forelimb diagram (right): black arrows = shoulder, white
 982 arrows = elbow; bones of left forelimb in lateral view. Shape key: circles = tridactyl Palaeotheriidae;
 983 triangles = tetradactyl Palaeotheriidae; square = Tapiridae; diamond = Lophiodontidae.

984



985

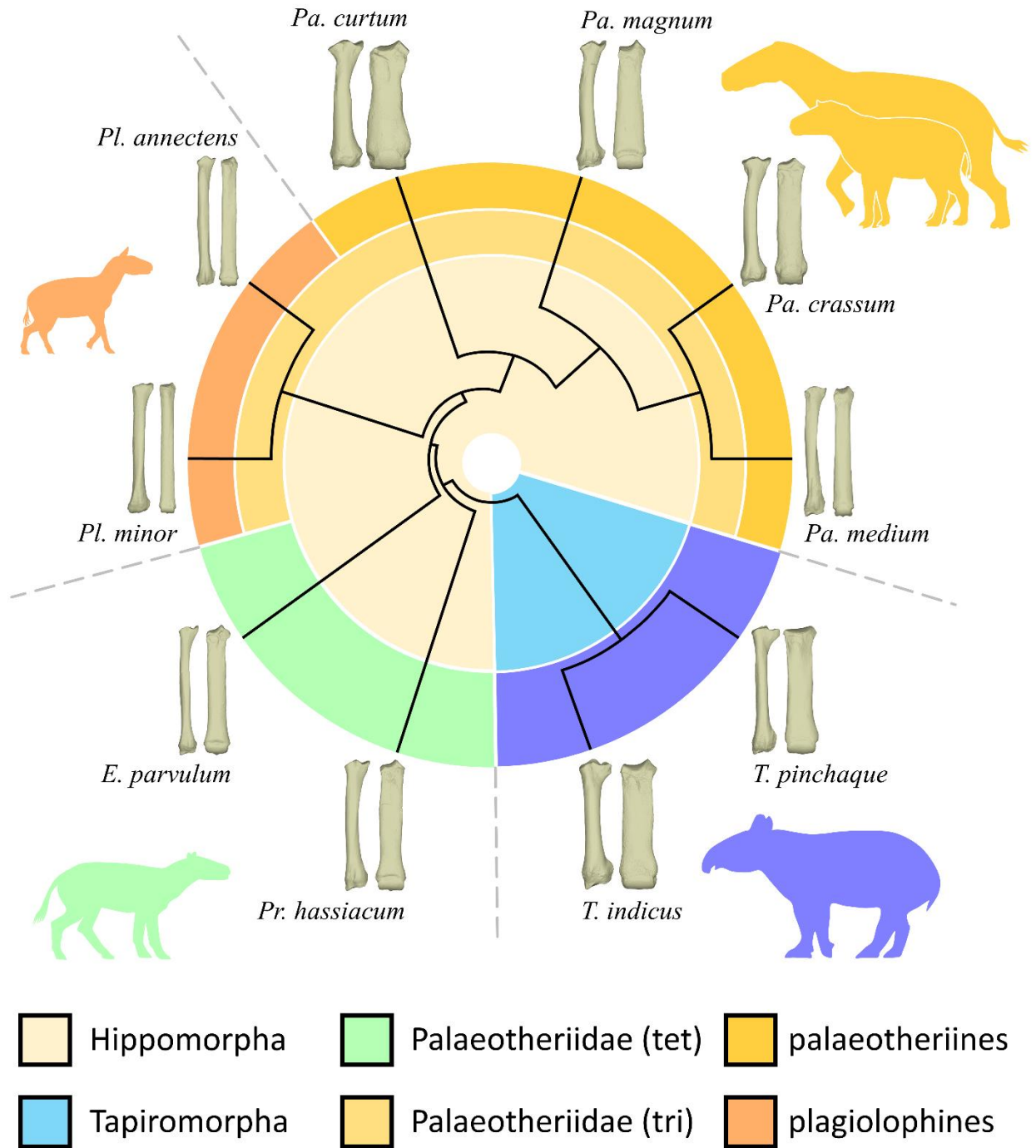
986 **Figure 5.** Long-bone ratio comparison of *Tapirus* spp. and selected extinct perissodactyls. **(a)** Radio-
 987 humeral (HR) and metacarpo-humeral (HMC) ratios plotted against one another. **(b)** Neighbour-
 988 joining trees based on distances between mean ratios for extant *Tapirus* and European perissodactyls
 989 (excluding *Plagiolophus* spp.). Dotted lines mark approximate boundary between cursorial and
 990 mediportal long-bone ratios, according to Gregory (1929). Silhouettes represent taxa demonstrating
 991 typically graviportal (Rhinocerotidae: *Teleoceras*) and cursorial (Palaeotheriinae: *Plagiolophus*) limb
 992 ratios.

993

994

995

996



997

998

Figure 6. Variation of locomotor morphology across Palaeotheriidae. Radius (left) and third

999

metacarpal shown for three clades of Palaeotheriidae alongside modern tapirs for comparison; bones

1000

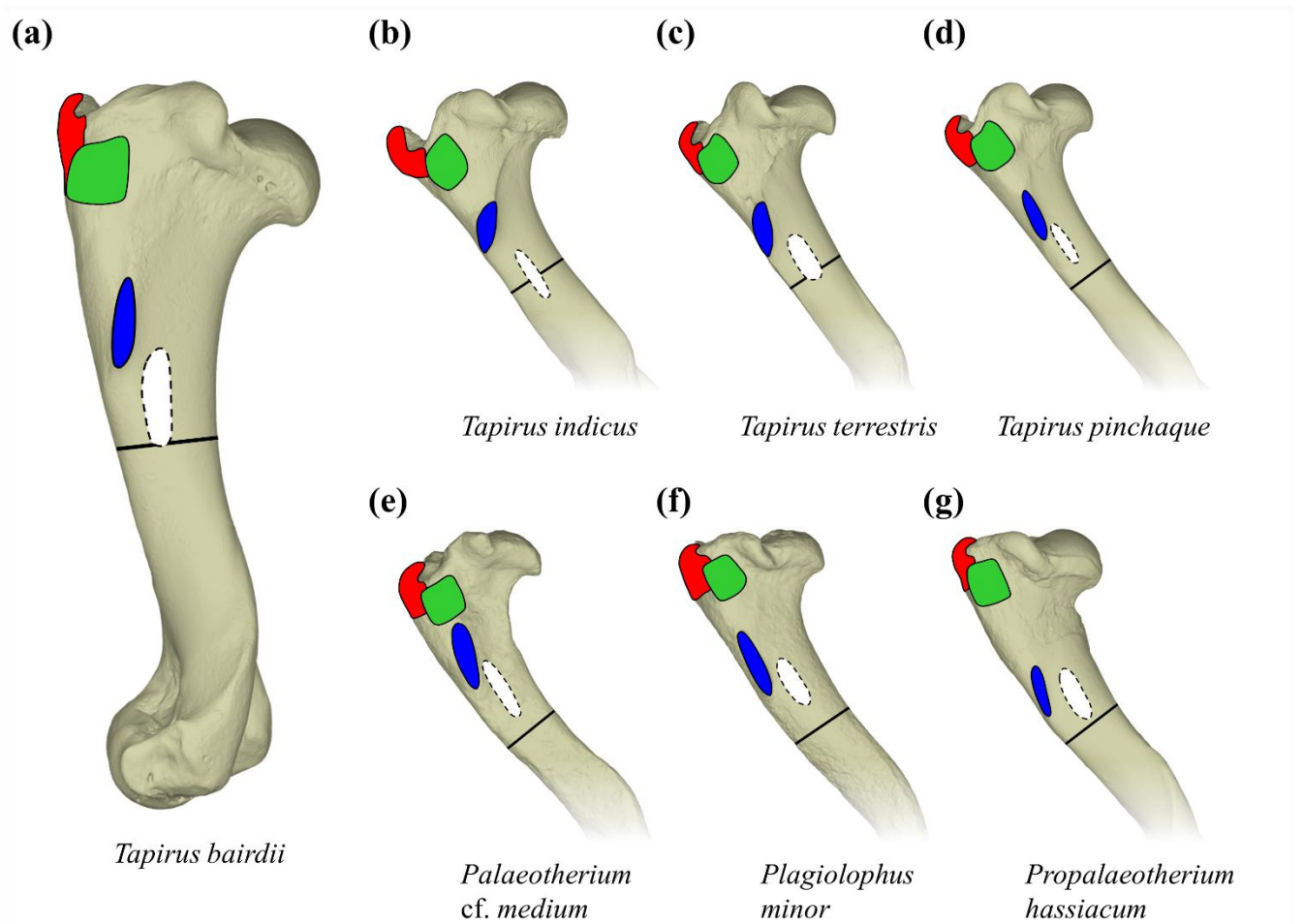
not to scale. Unrooted phylogeny based on Franzen (1992) and Danillo, et al. (2013). Silhouettes

1001

represent exemplar *bauplans* for each group. Abbreviations: tet = tetradactyl; tri = functionally

1002

tridactyl.



1003

1004

1005

1006

1007

1008

1009

1010

1011

1012

1013

Figure 7. Variation of muscular insertion sites on the humerus of tapirs and early European perissodactyls. Humeri of tapirs (a-d) shown alongside three palaeothere taxa (e-g) in lateral view. Black bar represents midpoint of the humeral shaft. Muscular insertions: *m. supraspinatus* (red); *m. infraspinatus* (green); *m. deltoideus* (blue); *m. teres major* (medial insertion; white). In particular note variation in teres major and deltoid insertions across *Tapirus* and between early European perissodactyls.

1014 **Table 1.** List of taxa included in this study. † = extinct; * = long-bone ratio only. Abbreviations: Eu
 1015 = Europe, SE As = South-East Asia, CAM = Central America, NAm = North America, SAm = South
 1016 America; Eo = Eocene, Oli = Oligocene, Mio = Miocene, Ple = Pleistocene, Hol = Holocene.

Higher Taxonomy	Species	Locality	Age
Tapiromorpha			
Tapiridae			
<i>Tapirus</i>	<i>bairdii</i>	C/SAm	Ple-Hol
<i>Tapirus</i>	<i>indicus</i>	SE As	Ple-Hol
<i>Tapirus</i>	<i>pinchaque</i>	SAm	Ple-Hol
<i>Tapirus</i>	<i>terrestris</i>	SAm	Ple-Hol
<i>Tapirus</i>	<i>polkensis</i> †	NAm	Mio
<i>Colodon</i> *	<i>occidentalis</i> †	NAm	Oli
Helaletidae* †			
<i>Heptodon</i> *	<i>calciculus</i>	NAm	Eo
<i>Heptodon</i> *	<i>posticus</i>	NAm	Eo
Lophiodontidae †			
<i>Paralophiodon</i>	<i>leptorhynchum</i>	Eu	Eo
<i>Lophiodon</i>	<i>remense</i>	Eu	Eo
<i>Lophiodon</i>	<i>tapirotherium</i>	Eu	Eo
Rhinocerotoidae*			
<i>Metamynodon</i> *	<i>planifrons</i> †	NAm	Oli
<i>Teleoceras</i> *	<i>major</i> †	NAm	Mio
<i>Teleoceras</i> *	<i>hicksi</i> †	NAm	Mio
<i>Uintaceras</i> *	<i>radinskyi</i> †	NAm	Eo
Indeterminate Tapiromorpha †			
<i>Chasmotherium</i> ^a	<i>minimus</i>	Eu	Eo
Hippomorpha			
Palaeotheriidae † (<i>generic prefix</i>)			
<i>Palaeotherium</i>	(<i>Pa.</i>) <i>magnum</i>	Eu	Eo
<i>Palaeotherium</i>	(<i>Pa.</i>) <i>medium</i>	Eu	Eo-Oli
<i>Palaeotherium</i>	(<i>Pa.</i>) <i>muelbergi</i>	Eu	Eo
<i>Palaeotherium</i>	(<i>Pa.</i>) <i>curtum</i>	Eu	Eo
<i>Palaeotherium</i>	(<i>Pa.</i>) <i>crassum</i>	Eu	Eo
<i>Palaeotherium</i>	(<i>Pa.</i>) <i>castrense</i>	Eu	Eo
<i>Plagiolophus</i>	(<i>Pl.</i>) <i>annectens</i>	Eu	Eo
<i>Plagiolophus</i>	(<i>Pl.</i>) <i>major</i>	Eu	Eo
<i>Plagiolophus</i>	(<i>Pl.</i>) <i>minor</i>	Eu	Eo-Oli
<i>Propalaeotherium</i>	(<i>Pr.</i>) <i>hassiacum</i>	Eu	Eo
<i>Propalaeotherium</i>	(<i>Pr.</i>) <i>isselanum</i>	Eu	Eo
<i>Propalaeotherium</i>	(<i>Pr.</i>) <i>voigti</i>	Eu	Eo
<i>Eurohippus</i>	(<i>Eu.</i>) <i>parvulum</i>	Eu	Eo
<i>Eurohippus</i> *	(<i>Eu.</i>) <i>messelensis</i>	Eu	Eo
Equidae †			
<i>Pliolophus</i>	<i>vulpiceps</i>	Eu	Eo
<i>Arenahippus</i> *	<i>grangeri</i>	NAm	Eo
<i>Mesohippus</i> *	<i>bairdii</i>	NAm	Eo-Oli
Indeterminate Equoidea †			

*Hallensia**matthesi*

Eu

Eo

1017 ^a*Chasmothorium minimus* (= *Hyrachyus minimus*) after Remy (2015)

1018 **Table 2.** Tukey WSD post-hoc results following ANOVAs of humerus, third metacarpal and unciform bone
 1019 shape variation along principal component 1 (PC1). Modern tapirs similar to extinct taxa in bold.

Species	N	Subset			
		1	2	3	4
Humerus (PC1 scores)					
<i>T. indicus</i>	8	-0.071			
<i>T. terrestris</i>	7		-0.035		
Lophiodontidae	3		-0.030		
<i>T. bairdii</i>	5		-0.019		
<i>T. polkensis</i>	4		-0.005		
<i>T. pinchaque</i>	4			0.032	
<i>Palaeotherium</i>	2			0.034	
<i>Plagiolophus</i>	8			0.054	0.054
<i>Propalaeotherium</i>	3				0.074
Metacarpal III (PC1 scores)					
<i>Plagiolophus</i>	16	-0.077			
<i>Eurohippus</i>	4		-0.038		
<i>Palaeotherium</i>	12		-0.028		
<i>Propalaeotherium</i>	11			0.007	
<i>T. polkensis</i>	8			0.021	
<i>T. pinchaque</i>	3			0.039	0.039
<i>T. terrestris</i>	6			0.043	0.043
<i>T. bairdii</i>	5				0.062
<i>T. indicus</i>	7				0.076
Unciform (PC1 scores)					
<i>T. polkensis</i>	6	-0.093			
<i>T. indicus</i>	6	-0.082			
<i>T. terrestris</i>	5	-0.071			
<i>T. bairdii</i>	5	-0.048			
<i>T. pinchaque</i>	4	-0.048			
<i>Chasmothorium</i>	2		0.013		
<i>Plagiolophus</i>	2		0.017		
<i>Propalaeotherium</i>	5		0.037		
<i>Palaeotherium</i>	3			0.086	
<i>Paralophiodon</i>	8				0.1671

1020

1021

1022

1023

1024

1025

1026

1027 **Table 3.** ANOSIM results comparing modern *Tapirus* spp. with early European perissodactyls, based on
 1028 Procrustes aligned shape coordinates for the humerus, third metacarpal and unciform. R-statistic between 0
 1029 and 1; 0 = equal within and between-group dissimilarity, 1 = between-group dissimilarity greater than all
 1030 within-group similarity interactions. PA= *Palaeotherium* spp.; PL = *Plagiolophus* spp., PR =
 1031 *Propalaeotherium* spp., EU = *Eurohippus*, LO = Lophiodontidae spp., CH = *Chasmootherium*.

Humerus						
	PA	PL	PR	LO		
<i>T. bairdii</i>	0.836	0.815	0.908	1		
<i>T. indicus</i>	0.978	1	1	1		
<i>T. pinchaque</i>	0.821	0.831	0.685	1		
<i>T. terrestris</i>	0.896	0.950	0.956	0.996		
Metacarpal III						
	<i>Pa. magnum</i>	<i>Pa. crassum</i>	<i>Pa. medium</i>	PL	PR	EU
<i>T. bairdii</i>	0.939	0.959	1	1	1	1
<i>T. indicus</i>	0.980	1	1	1	1	1
<i>T. pinchaque</i>	0.593	0.741	1	1	1	1
<i>T. terrestris</i>	0.897	0.925	1	1	1	1
Unciform						
	PA	PL	PR	CH	LO	
<i>T. bairdii</i>	0.610	1	0.920	1	1	
<i>T. indicus</i>	0.803	1	0.997	1	1	
<i>T. pinchaque</i>	0.444	0.964	0.888	0.821	1	
<i>T. terrestris</i>	0.651	1	0.956	1	1	

1032

1033

1034

1035

1036

1037

1038

1039

1040

1041

1042

1043

1044

1045 **Table 4.** Long-bone ratios and estimated body masses for tapirs and early European perissodactyls.1046 * = predicted based on sister taxa. **N** = number of articulated specimens; (n) = total specimens for1047 average. **HR** = radius/humerus; **HMC** = third metacarpal/humerus; **BM** = mean estimated body

1048 mass.

Genus	Species	N (n)	HR	HMC	BM (kg)
<i>Tapirus</i>	<i>bairdii</i>	5 (5)	84.6	46.9	228.7
<i>Tapirus</i>	<i>indicus</i>	7 (8)	89.4	47.6	326.4
<i>Tapirus</i>	<i>pinchaque</i>	4 (4)	83.5	47.1	202.4
<i>Tapirus</i>	<i>terrestris</i>	7 (7)	86.1	48.8	216.6
<i>Tapirus</i>	<i>polkensis</i>	2 (15)	96.8	54.5	116.9
<i>Paralophiodon</i>	<i>leptorhynchum</i>	1 (1)	87.45	45.4	232.5
<i>Chasmothorium</i>	<i>minimus</i>	1 (2)	86.9	49.9	-
<i>Palaeotherium</i>	<i>magnum</i>	1 (4)	93.7	49.8	240.3
<i>Plagiolophus</i>	<i>major</i> *	0 (5)	107.5*	62.9	78.9
<i>Plagiolophus</i>	<i>annectens</i>	0 (6)	117.0	72.8	34.8
<i>Plagiolophus</i>	<i>minor</i>	0 (11)	126.6	82.1	19.3
<i>Propalaeotherium</i>	<i>hassiacum</i>	0 (24)	93.3	48.6	46.5
<i>Propalaeotherium</i> ^a	<i>voigti</i>	0 (4)	96.4	56.9	23.0
<i>Eurohippus</i>	<i>parvulum</i>	1 (6)	90.5	52.2	-
<i>Eurohippus</i> ^b	<i>messelensis</i>	2 (2)	88.2	49.6	-
<i>Hallensia</i> ^c	<i>matthesi</i>	1 (1)	93.5	55.1	-

1049

1050 References: ^a Franzen (2010); ^b Franzen & Hauptzeter (2017); ^c Franzen (1990)

1051